Replication-transcription conflicts trigger extensive DNA degradation in *Escherichia coli* cells lacking RecBCD

Juachi U. Dimude, Sarah L. Midgley-Smith and Christian J. Rudolph*

*Corresponding author: christian.rudolph@brunel.ac.uk

Division of Biosciences, College of Health and Life Sciences,
Brunel University London, Uxbridge, UB8 3PH, UK

ABSTRACT

Bacterial chromosome duplication is initiated at a single origin (*oriC*). Two forks are assembled and proceed in opposite directions with high speed and processivity until they fuse and terminate in a specialised area opposite to *oriC*. Proceeding forks are often blocked by tightly-bound protein-DNA complexes, topological strain or various DNA lesions. In *Escherichia coli* the RecBCD protein complex is a key player in the processing of double-stranded DNA (dsDNA) ends. It has important roles in the repair of dsDNA breaks and the restart of forks stalled at sites of replication-transcription conflicts. In addition, *ΔrecB* cells show substantial amounts of DNA degradation in the termination area. In this study we show that head-on encounters of replication and transcription at a highly-transcribed *rrn* operon expose fork structures to degradation by nucleases such as SbcCD. SbcCD is also mostly responsible for the degradation in the termination area of *ΔrecB* cells. However, additional processes exacerbate degradation specifically in this location. Replication profiles from *ΔrecB* cells in which the chromosome is linearized at two different locations highlight that the location of replication termination can have some impact on the degradation observed. Our data improve our understanding of the role of RecBCD at sites of replication-transcription conflicts as well as the final stages of chromosome duplication. However, they also highlight that current models are insufficient and cannot explain all the molecular details in cells lacking RecBCD.

INTRODUCTION

All organisms require the accurate duplication of their genome and the faithful transmission of all resulting copies into the daughter cells [1]. Any impairment of these processes can potentially be fatal for cells or result in mutations and genomic instability, an important driver for the development of cancer and the cause of several human syndromes [2]. In the bacterium *Escherichia coli* DNA replication of the single circular chromosome initiates at a single origin (*oriC*). The initiator protein DnaA facilitates the assembly of two replication fork complexes (replisomes), which move away from *oriC* in opposite directions with high speed and accuracy [3]. Replication is completed when converging forks fuse opposite *oriC* in an area that contains a specialised termination region flanked by polar *ter* sequences (*terA–J*) [4,5]. If bound by Tus terminator protein, the resulting *ter*/Tus complexes form a strong replication fork pause site [4,6]. The polar *ter* sites are oriented such that they allow forks to enter but not to leave the termination area. The chromosome is therefore divided into two approximately equal halves called replichores, each replicated by a single replication fork complex coming from *oriC* [7].

But progression of the replisomes from *oriC* to the termination area is not always smooth, as they will encounter a variety of barriers [8–10]. Besides various forms of spontaneous DNA damage, both topological strain and tightly-bound protein-DNA complexes are likely to interfere with the duplication process. Replication and transcription use the same template, and transcribing RNA polymerase complexes provide not only substantial nucleoprotein barriers to fork movement due to their very high affinity [8], but also topological challenges due to the positive supercoiling ahead of and negative supercoiling behind the transcription bubble [11,12]. Head-on

encounters of DNA replication and transcribing RNA polymerase complexes have been identified as particularly problematic [5,13–17]. However, especially high levels of transcription are likely to interfere with replication even if both processes are proceeding co-directionally [13,18].

Several mechanisms aid the progression of DNA replication through tightly bound protein-DNA complexes. In *E. coli* helicases such as Rep, UvrD and DinG promote fork progression through nucleoprotein complexes [17,19,20]. Rep physically associates with the replicative helicase DnaB and for this reason is considered an accessory replicative helicase [21,22]. In the absence of Rep, chromosome duplication takes almost twice as long as in wild type cells [19,20,23]. In addition, enzymes involved in homologous recombination can assist replication fork movement through highly transcribed areas [9,24,25]. In *E. coli* RecBCD was shown to be essential for viability under fast growth conditions in strains in which an *rrn* operon was inverted to force head-on encounters of replication and transcription, [14]. RecBCD is a protein complex which possesses both nuclease and helicase activities [24]. It binds to double-stranded DNA (dsDNA) that is blunt or near blunt [24]. The RecB and RecD subunits are helicases with opposite polarities: RecB translocates in a 3' to 5' direction while RecD translocates in a 5' to 3' direction [24]. Upon binding of a dsDNA end RecBCD unwinds and degrades DNA with high speed and processivity, both *in vitro* and *in vivo* [24,26] until a *chi* site, an asymmetric octamer sequence, is recognised [27]. Recognition of a *chi* site triggers the inhibition of the degradation of the 3' end, which causes the RecBCD complex to produce a 3' ssDNA overhang suitable for the loading of RecA recombinase [28].

While accessory helicases are thought to target active but paused replisomes, recombination enzymes are likely to process blocked fork structures where the replisome is not active any more [29]. Thus, a situation where an accessory helicase is required is likely to differ significantly from a situation where recombination proteins such as RecBCD are necessary. In line with this idea, *E. coli* cells lacking either RecBCD or Rep are viable but *Δrep ΔrecB* cells were shown to be synthetically lethal [30,31].

More recently an additional phenotype of cells lacking RecBCD became apparent. The analysis of replication profiles of *ΔrecBCD ΔthyA* cells undergoing thymine starvation revealed a substantial depletion of marker frequency within the terminus region of the chromosome, leading to the suggestion that progression of the replication forks towards the terminus region might be severely inhibited [32]. Replication profiles generated via high resolution marker frequency analysis from Deep Sequencing showed that this depletion of sequences in the termination area is also observed in *ΔrecBCD* cells under fast growth conditions [33] and can be modulated by the inactivation of the nucleases SbcCD and ExoI (encoded by *xonA*) [34,35]. In addition, septum closure was shown to play an important role in triggering the depletion of sequences, suggesting that degradation of DNA, rather than the inability of replication forks to reach the termination area, is mainly responsible for the depletion observed [34,36]. The tracking of a fluorescently tagged region within the termination area revealed that, following an initiating event specific to cells lacking RecBCD, one daughter cell is generated that loses sequences of the terminus region and will not generate a viable daughter cell again, while the second cell retains a complete terminus region. This process is "inherited", as the latter cell will generate once again one cell in

which sequences of the terminus region is lost and a second cell retaining the terminus region [34,36], suggesting that surviving cells retain a defect despite the termination area being intact. The data have led to a model in which one broken replication fork near the terminus region triggers formation of a chromosome with one linear dsDNA end, while the structure of the second replication fork remains intact. If not repaired this leads to a situation which is reminiscent of rolling-circle replication, retaining one circular chromosome in one cell and generating yet again a linear chromosome. Segregation problems of this linear chromosome then lead to guillotining of the damaged chromosome [25,34,36]. This model is able to explain in particular why after an initiating event one cell is generated in which degradation of the terminus region is observed and which is inviable, whereas the second cell is viable but retains a defect that triggers the same aberrant pattern in the next generation [25,34,36].

In this study we have further analysed replication dynamics and DNA degradation in cells lacking RecBCD. We show that in *oriC*$^+$ *oriZ*$^+$ *ΔrecB* cells in which replication is initiated at *oriC* as well as an additional ectopic replication origin, forks traversing in a direction opposite to normal are not able to proceed after encountering an *rrn* operon head-on, with little indication of forks being arrested elsewhere. Forks arrested trigger degradation by nucleases such as SbcCD, which is persistent enough to significantly interfere with firing of the ectopic origin more than 100 kb away. No such degradation is seen in cells lacking Rep helicase, in which DNA replication is also severely blocked after encountering an *rrn* operon head-on. Our data show that SbcCD is also the nuclease that is responsible for the majority of the degradation in the terminus region of *ΔrecB* cells. However, in contrast to the situation at *rrn* operons, inactivation of SbcCD only reduces the extent of degradation, but does not abolish it, in line with the idea that a different process, such as septum formation, contributes to the DNA degradation observed [25,34,36]. Replication profiles from *ΔrecB* cells in which the chromosome is linearized at two different locations highlight that the termination point of forks can have some impact degradation. The data presented enhance our understanding of the role of RecBCD, both at replication-transcription conflicts and at the final stages of chromosome duplication, but they also highlight that current models are not yet capable of fully explaining the events in cells lacking RecBCD.

MATERIALS & METHODS

Bacterial strains, growth media and general methods

For *Escherichia coli* K12 strains see Supplementary Table 1. Strains were constructed via P1*vir* transductions [37] or by single-step gene disruptions [38]. For details of growth media see Supplementary Methods.

Synthetic lethality assay

The synthetic lethality assay was performed as described [39,40]. In essence, a wild type copy of a gene of interest (*recB*, *rep*) under its native promoter was cloned into pRC7, a *lac*$^+$ mini-F plasmid that is rapidly lost, and used to cover the deletion of the same gene in the chromosome in a *Δlac*$^-$ background. Additional mutations can then be introduced to test for synthetic lethality

with the deleted allele. If synthetically lethal, cells that lose the plasmid will fail to grow and only *lac*$^+$ colonies formed by cells retaining the plasmid will be observed. When viability is reduced but not eliminated, colonies formed by cells retaining the plasmid are noticeably larger than white colonies formed by plasmid-free cells. Cultures of strains carrying the relevant pRC7 derivatives were grown overnight in LB broth containing ampicillin to maintain plasmid selection, diluted 100-fold in LB broth and grown without ampicillin selection to an A_{600} of 0.4 before spreading dilutions on LB agar or M9 glucose minimal salts agar supplemented with X-gal and IPTG. Plates were photographed and scored after 48 h (LB agar) or 72 h (M9 agar) at 37°C. At least two independent experiments were performed for each construct investigated.

Marker frequency analysis by deep sequencing

Marker frequency analysis by deep sequencing was performed as described before [13]. See the Supplementary Methods section for a detailed description. Replication profiles of all key constructs were confirmed by two independent experiments.

Linearization of the *E. coli* chromosome

Linearization of the *E. coli* chromosome was performed as described before [33,41]. See Supplementary Methods and Suppl. Figure 1 for further details.

RESULTS

Escherichia coli cells lacking RecBCD show a marked underrepresentation of sequences in the terminus region of the chromosome [33,42]. A recent analysis of this effect strongly suggests that the underrepresentation is caused by the degradation of chromosomal DNA, rather than an inability of forks to complete chromosome duplication [34,36]. The analysis of replication profiles in strains deficient for both RecBCD and the 3' exonucleases ExoI and SbcCD has demonstrated that the extent of degradation observed in *ΔrecB* cells is much reduced if both ExoI and SbcCD are missing [35,36], in line with the observation that the combined inactivation of ExoI and SbcCD is able to suppress the defects in DNA recombination, repair, and viability of *ΔrecBC* cells [43,44]. However, both recent studies only show replication profiles of *ΔrecB* cells in which both ExoI and SbcCD are inactivated [35,36].

The extent of DNA degradation in the terminus area of *recB* cells mostly depends on SbcCD

Cells lacking both ExoI (encoded by *xonA*) and SbcCD [45], but in particular cells lacking ExoI, SbcCD and ExoVII (encoded by *xseA*) showed dramatic over-replication of the termination area [33]. To investigate the effects of the inactivation of these exonucleases on the degradation in *ΔrecB* cells more systematically, we analysed the replication profiles of *ΔrecB ΔxonA*, *ΔrecB ΔxseA* and *ΔrecB ΔsbcCD* double mutants. We found that while the inactivation of both ExoI and ExoVII had little effect on the degradation of the terminus region in *recB* cells (Figure 1 ii & iii), deletion of *sbcCD* showed a marked effect (Figure 1 iv). The "valley" caused by the degradation is extremely narrow in *ΔrecB ΔsbcCD* cells. The addition of a *ΔxonA* mutation does not change the

replication profile of *ΔrecB ΔsbcCD* cells significantly (Figure 1 v). The valley appears slightly wider than in *ΔrecB ΔsbcCD* cells, but given that replication profiles suffer from some variability (see Suppl. Methods) we are currently not able to determine whether the degradation observed in *ΔrecB ΔsbcCD* and *ΔrecB ΔsbcCD ΔxonA* cells is significantly different. Nevertheless, as observed before [35,36], the loss of sequences in the area around the *dif* site is as extreme in *ΔrecB ΔsbcCD* (*ΔxonA*) cells as it is in *ΔrecB* single mutants (cf. Figures 1 i & 1 iv). This strongly suggests that SbcCD, while mainly responsible for the extent of the degradation of DNA in the termination region of *ΔrecB* cells, is not responsible for the event that initiates the degradation. As a genetic interaction between *recB* and *recJ* was reported before [14], we also wanted to investigate the effect of a *recJ* deletion on the degradation in the termination area in *ΔrecB* cells. As shown in Figure 1 vi the replication profile of *ΔrecB ΔrecJ* cells suggests that RecJ might be responsible for some degradation, but the effect observed is mild in comparison to the deletion of *sbcCD*.

Effect of *rpo** and chromosome linearization on the degradation in the termination area of *recB* cells

What might initiate degradation in the termination area? Using an approach similar to that described by Sinha and colleagues [36] we investigated whether the fusion of the two replisomes might be responsible for the initiation of DNA degradation in *ΔrecB* cells. To prevent replication forks from fusing, we linearized the *E. coli* chromosome near the *dif* site [41], an approach successfully used before to show that the over-replication of the termination area in cells lacking RecG is much reduced if the fusion of replisomes is prevented [33,46]. To achieve linearization the linearization site *tos* from bacteriophage N15 was integrated into the E. coli chromosome near dif. Upon lysogenic infection of these cells with N15, expression of the phage telomerase TelN cleaves and processes *tos*, thereby generating a linear chromosome with two hairpin ends (Suppl. Figure 1). Chromosome linearization of our *ΔrecB* construct resulted in the same striking asymmetry (Figure 2 v) as observed by Sinha and co-workers [36]. While degradation of the left-hand replichore is prominently visible, degradation of the right-hand replichore is much reduced. It is noteworthy that the *dif* dimer resolution site is located in the non-degraded chromosomal end, demonstrating that recombination at *dif* is not responsible for triggering the DNA degradation observed, as reported [34].

The asymmetry of degradation observed upon linearization of the chromosome could fit with a defined location where degradation is started. Linearization would then restrict degradation to the chromosome end that contains the location where degradation is started, while it would prevent degradation of the other end. A closer analysis of the replication profile of *ΔrecB* cells showed that the low point is located in a chromosomal area with genes that have little to do with DNA replication and repair or which are not fully characterised. The only obvious candidate genes were the *hipA* and *hipB* genes. The *hipBA* system is a toxin/antitoxin module. Expression of *hipA* was shown to activate ppGpp synthesis by RelA [47], which in turn leads to growth arrest due to inhibition of protein, RNA, and DNA synthesis [48]. DNA loss observed in the termination area of *ΔhipA ΔrecB* and especially in *ΔhipB ΔrecB* cells was larger than in *ΔrecB* single mutants

(Figure 3 iii & iv) as reported [34]. Thus, neither the *hipAB* gene products nor their coding sequences are responsible for initiation of the DNA degradation observed in *recB* cells.

One of the effects of ppGpp is the modulation of RNA polymerase (RNAP). ppGpp binds next to the active site of RNAP and destabilises the open complexes [49,50]. The toxicity of HipA is normally counteracted by its binding partner HipB, a transcriptional repressor [51,52]. Thus, the particularly pronounced degradation observed in *ΔhipB ΔrecB* cells could be caused by RNA polymerase being less stably bound due to increased ppGpp levels, thereby allowing more processive DNA degradation by SbcCD. If so then introduction of a subclass of stringent RNAP mutations called *rpo** should result in a similar widening of the degradation of the termination area, as *rpo** mutations mimic the effect of ppGpp [53,54]. This was precisely what we observed. DNA degradation of the termination area in *ΔrecB rpo** cells was significantly wider, very reminiscent of the degradation observed in *ΔhipB ΔrecB* cells (Figure 3 v). Thus, our data are in line with the idea that widening of the DNA degradation observed in *ΔhipB* cells is at least in part caused by the destabilisation of RNA polymerase via ppGpp. Because little effect of an *rpo** mutation on the degradation in the termination area is seen in *ΔrecB ΔsbcCD* cells (Figure 3 vi) it seems that tight protein-DNA complexes might interfere specifically with SbcCD-dependent degradation of DNA.

To further investigate whether degradation might be caused by a defined initiation point we used a strain in which the linearization site is moved to a different location. If the DNA degradation observed is caused by a defined initiation point, shifting the linearization point further into the non-degraded arm of the chromosome should cause no major change of the replication profile, as linearization should still protect the left-hand replichore from being degraded. To test this we used a construct in which the linearization site is shifted 200 kb away from *dif* into the left-hand replichore [41]. Because replication coming from *oriC* will have to proceed through both *terC* and *terB* in this construct to reach the end of the chromosome, the experiment required us to also delete *tus*, as described [41]. Strikingly, the replication profile of this construct revealed significant degradation of both chromosomal ends (Figure 2 vi). Linearization of the chromosome was confirmed both via PCR and pulsed-field gel electrophoretic analysis of high molecular weight chromosomal DNA (Suppl. Figure 1). In addition, the replication profile shows a very clear shift of the low-point from near *dif* in non-linearized constructs to the location of the +200 kb linearization site (Figure 2 vi), providing additional confirmation of the successful linearization of the chromosome.

The fact that a shift of the linearization point restores a symmetrical degradation pattern strongly argues that DNA degradation is not triggered at a defined location. Instead, it appears that in *ΔrecB* cells with the chromosome linearized near *dif*, degradation is prevented by some feature of the left-hand replichore. Both the *hipAB* and *rpo** results are in line with the idea that degradation might be modulated by protein-DNA complexes and a significant difference between linearization near *dif* and at the +200 kb site in the presence and absence of Tus protein, respectively. To investigate whether the relatively close proximity of the linearization point to *ter*/Tus complexes at *terC/B* might interfere with DNA degradation, we analysed the replication profile in a *ΔrecB Δtus* background in which the chromosome was linearized near the *dif* site. We

expected that the absence of *ter*/Tus complexes in close proximity of the linearization site would re-establish degradation in both chromosome ends. However, the replication profile remained asymmetric, despite the inactivation of the replication fork trap (Figure 2 viii). Thus, we currently do not know what factor might be protecting the left-hand replichore from degradation in *recB* cells in which the chromosome is linearized near *dif*.

Replication dynamics in *recB* cells with an additional ectopic replication origin

In order to investigate whether the degradation might be triggered by the processing of replication forks as they terminate we used cells in which a second ectopic origin, *oriZ*, was integrated into the chromosome [13,55]. One big difference between wild type and *oriC*$^+$ *oriZ*$^+$ cells is that replication forks coming from *oriZ* travelling clockwise will reach the replication fork trap much earlier than forks coming from *oriC* travelling counter clockwise. Upon deletion of *tus* the forks coming from *oriZ* will escape the termination area and proceed into the opposite replichore, forming a termination point roughly equidistant from both *oriC* and *oriZ* (Figures 4 i & 4 ii) [13]. Thus, if degradation in the absence of RecBCD is triggered by fusing forks, the area of degradation should be shifted together with the fork fusion point in *oriC*$^+$ *oriZ*$^+$ *Δtus ΔrecB* cells. In addition, introduction of a second ectopic replication origin also establishes a second and ectopic termination area between *oriC* and *oriZ*, with forks fusing between the *rrn* operons *E* and *H* (Figure 4 i) [13]. If fusing forks in general cause degradation in the absence of RecBCD this should be visible in the ectopic termination area.

While both origins fire with similar frequency in *oriC*$^+$ *oriZ*$^+$ cells (Figure 4 i), the peak height of the ectopic *oriZ* is markedly decreased in *oriC*$^+$ *oriZ*$^+$ *ΔrecB* cells (Figure 4 iii), suggesting that it fires with a much reduced frequency in comparison to *oriC,* at least on a population basis. In addition, the ectopic fork fusion location is significantly skewed. Forks coming from *oriZ* appear to be unable to proceed past *rrnH* (Figure 4 iii). However, the low point of the replication profile in the native termination region of the chromosome proved to be precisely in the same location, regardless of the presence or absence of Tus (Figure 4 iv), and the extent of DNA degradation was identical (Figure 4 ivb).

The lack of change of the location of the fork fusion point is most likely explained by the reduced firing of the ectopic *oriZ*. If the frequency of *oriZ* firing is low then forks will mostly initiate at the native *oriC*, which means the majority of fork fusion events will take place opposite in the native termination area, regardless of the presence or absence of Tus [5]. Any mild distortion of the replication profile by a small number of forks coming from *oriZ* is likely to be obscured by the DNA degradation in the termination area.

The shift of the termination point in the ectopic fork fusion location is more informative. The termination point forms a defined valley with the low-point at *rrnH,* with little indication that any fork fusion events are taking place at the original fork fusion site at ~4.45 Mbp (cf. Figures 4 i & 4 iii). RecBCD has been implicated in the processing of replication forks stalled at sites of replication-transcription conflicts [10,14]. If *rrnH* permanently blocks progression of replication forks coming from *oriZ* going in a direction opposite to normal in the absence of RecBCD, this

might explain the reduced *oriZ* peak height, because the permanent arrest of forks in relative proximity to *oriZ* will limit its capacity for firing.

To investigate whether *rrnH* constitutes a strong block to DNA replication in the absence of RecB we tried to delete the native *oriC* in *oriC*$^+$ *oriZ*$^+$ *ΔrecB* cells. If forks coming from *oriZ* are permanently blocked at or near *rrnH*, *ΔoriC oriZ*$^+$ *ΔrecB* cells should be inviable, as the second fork would be arrested in the native termination area. This is indeed what we observed (Figure 5). We found that *oriC* could only be deleted if *recB* was expressed in trans from a pRC7 plasmid carrying the wild-type *recB* gene. pRC7 is an unstable plasmid that contains a copy of the *lac* operon. It is rapidly lost if selection is not maintained. In a strain deleted for the chromosomal *lac* operon, the presence or absence of the plasmid can be detected on agar plates containing the beta-galactosidase indicator X-gal. Blue colonies show the presence of the plasmid (*lac*$^+$), while white colonies show the absence of the plasmid. White sectors within blue colonies can be observed if plasmid loss occurs after plating [39,40]. This assay revealed that plasmid-free *ΔoriC oriZ*$^+$ *ΔrecB* cells were unable to form colonies (Figure 5 xi). This observation demonstrates that when the chromosome is replicated exclusively from the ectopic replication origin *oriZ*, the RecBCD complex becomes essential for viability, in line with previous results [14].

Previous studies revealed that deletion of *oriC* from wild type cells carrying an ectopic origin (*oriZ*) compromises viability, leading to a much slower doubling time and the rapid accumulation of suppressor mutations [5,13]. This slow growth of *ΔoriC oriZ*$^+$ cells is partially suppressed by a) the inactivation of the replication fork trap or b) an *rpoB*35* point mutation, which reduces the stability of RNA polymerase-DNA complexes, thereby alleviating conflicts between replication and transcription [13]. To investigate whether the block of a replisome in the termination area at *ter*/Tus complexes creates a problem in cells lacking RecBCD we investigated whether *oriC* could be deleted from *oriC*$^+$ *oriZ*$^+$ *ΔrecB* cells if *tus* was deleted. This was not the case. As shown in Figure 5 xv, the deletion of the native origin in *oriC*$^+$ *oriZ*$^+$ *Δtus ΔrecB* cells did not result in viable colonies. Instead, the blue colonies observed showed noticeable size variations indicative of the presence of spontaneous suppressor mutations. This suggests that, rather than improving viability, the deletion of *tus* might make *ΔoriC oriZ*$^+$ *ΔrecB* cells more sick, despite the fact that the *recB* deletion is covered by a *recB*$^+$ plasmid.

If replication-transcription clashes are responsible for the fork block at *rrnH* then an *rpo** point mutation should partially suppress the lethality, as observed for *ΔoriC oriZ*$^+$ cells [13]. However, the synthetic lethality assay showed only subtle effects. On LB broth *ΔoriC oriZ*$^+$ *ΔrecB rpo** cells remained inviable (Figure 5 xiii). If grown on minimal salts medium the white colonies observed grew more robustly (cf. Figures 5 xii & 5 xiv), indicating that under slow growth conditions an *rpo** mutation somewhat improves the viability of *ΔoriC oriZ*$^+$ *ΔrecB* cells.

A mild positive effect of an *rpo** point mutation was also noticeable when we analysed the replication profiles of *oriC*$^+$ *oriZ*$^+$ *ΔrecB rpo** cells. As already observed in *ΔrecB* single origin cells (Figure 3 v) the *rpo** mutation led to a significant widening of the DNA degradation in the termination area (Figure 4 v). In addition we observed that the ectopic *oriZ* showed a significantly increased peak height. While DNA synthesis is still strongly blocked at *rrnH*, the almost horizontal marker frequency between *rrn* operons *H* and *E* suggests that replication can proceed

through *rrnH*, albeit at a low frequency and/or with a slow speed, in line with the mild improvement observed in our synthetic lethality assay (Figure 5).

The right-hand replichore of the *E. coli* chromosome contains 5 of the 7 highly transcribed *rrn* operons. We therefore repeated the experiments with a strain in which an ectopic replication origin called *oriX* was integrated into the left-hand replichore. Replication forks initiated at *oriX* and traversing counter clockwise will proceed through the termination area before being blocked at the first *ter*/Tus complex encountered in blocking orientation, which results in the clearly visible step of the replication profile at *terA* (Suppl. Figure 2 i). Upon deletion of *recB* we once again observed a substantial reduction of the *oriX* peak height, an effect that is also suppressed if an *rpo** mutation is introduced (Suppl. Figures 2 ii & 1 iii).

DNA degradation in *recB* cells at sites of replication-transcription conflicts

If the reduction of the peak height of the ectopic origin is caused by the arrest or collapse of forks in relatively close proximity to the origin then we should observe a similar reduction in peak height in other mutants known to struggle with replication-transcription conflicts. To test this we generated replication profiles of *oriC*$^+$ *oriZ*$^+$ cells lacking Rep helicase, a protein important for aiding the progression of replisomes through transcribed regions of the chromosome [19,20,23]. The mean speed of replication fork movement in *Δrep* cells is significantly reduced in comparison to wild-type cells [19,23]. This is reflected in the increased origin/terminus ratio observed in the replication profile of *Δrep* single mutants (cf. Figures 6A i & 6A ii). As expected, the native origin could not be deleted in *oriC*$^+$ *oriZ*$^+$ *Δrep* cells unless an *rpo** point mutation was introduced (Figures 6B vii & 6B ix); *ΔoriC oriZ*$^+$ *Δrep rpo** cells grew robustly, both on LB broth and minimal salts media. The replication profiles of *oriC*$^+$ *oriZ*$^+$ *Δrep* cells confirmed that the majority of forks arrested at *rrnH* (Figure 6A iv). Some forks were able to proceed, but either the speed of these forks is very slow or the fraction of forks being able to proceed is low or both. However, in contrast to our prediction we noticed that the peak height of the ectopic *oriZ* is almost as high as the peak height of *oriC* (Figure 6A iv). Upon introduction of an *rpo** point mutation, replication appears to be able to proceed with relative ease beyond *rrnH* and peak heights of *oriC* and *oriZ* were almost identical (Figure 6A v).

Why then is peak height of the ectopic origins in the absence of RecBCD so much reduced? RecBCD has not been implicated in origin activity and if the majority of forks coming from *oriZ* are stopped at *rrnH* in both *ΔrecB* and *Δrep* cells, both should exhibit a similar activity of *oriZ*. So what is causing the difference between *ΔrecB* and *Δrep* cells? Given the observation that SbcCD degrades DNA extensively in the absence of RecBCD in the termination area, we contemplated whether a similar type of degradation might be responsible for the reduced peak height. If forks stalled at *rrnH* are degraded by exonucleases towards *oriZ* in the absence of RecBCD this would limit the capacity of *oriZ* to fire. If so, peak heights of *oriC* and *oriZ* should be similar in *oriC*$^+$ *oriZ*$^+$ *ΔrecB ΔsbcCD* cells. This is precisely what we observed. Peak heights of *oriC* and *oriZ* were identical, with a dramatic drop of marker frequency towards *rrnH* (Figure 7 iii). Thus, it appears that, despite the presence of the accessory helicase Rep, head-on replication-transcription encounters at highly-transcribed genes require processing by RecBCD, as suggested [10,14]. In

the absence of RecBCD, fork structures become accessible to nucleolytic degradation and the data presented suggest that SbcCD is a key player for this degradation. However, it will require a more extensive analysis to verify whether and how much other exonucleases contribute.

DISCUSSION

In this study we show that the absence of RecBCD causes degradation of DNA by exonucleases such as SbcCD and RecJ in at least two different situations, namely in the termination area of the chromosome and at sites of severe replication-transcription conflicts. A variety of proteins have been suggested to facilitate progression of replication forks through areas with persistent protein-DNA complexes, including the helicases Rep, UvrD and DinG and RecBCD helicase/exonuclease [14,17,19,20,29]. Rep helicase, which was shown to promote fork movement through nucleoprotein complexes, appears to have a prominent role, as its absence results in at least a two-fold increase in the time needed to duplicate a chromosome [17,19,20,23]. In cells carrying inverted *rrn* operons RecBCD helicase/exonuclease was required for viability [14,17] and a combination of *rep* and *recBC* mutations was shown to be synthetically lethal [30], highlighting the interaction between Rep and RecBCD. However, in contrast to *Δrep*, *ΔrecB* cells do not show an extensive delay of chromosome duplication [29].

In line with these observations, our analysis of the replication profiles of *Δrep* and *ΔrecB* cells suggests very different replication issues. Cells lacking Rep helicase showed an overall increase of the origin/terminus ratio, without much indication of specific areas causing particular problems (Figure 6A). *rrn* operons encountered by replication in an orientation opposite to normal block the progression of synthesis and *oriZ*$^+$ *Δrep* cells cannot survive in the absence of the native origin (Figure 6B). However, some replisomes are able to proceed, and robust viability is restored if replication-transcription conflicts are lessened by an *rpo** point mutation (Figure 6B).

rrn operons encountered in an orientation opposite to normal in cells lacking RecBCD appear to be a hard block to replication, with no indication of replisomes proceeding past the *rrn* operon (Figure 4). Introduction of an *rpo** point mutation causes some alleviation, as viability of *ΔoriC oriZ*$^+$ *ΔrecB* is improved if grown in minimal salts medium (Figure 5), but *ΔoriC oriZ*$^+$ *ΔrecB rpo** cells remain inviable on LB broth (Figure 5) and the replication profiles confirm that forks proceed past *rrnH* with a low frequency, low speed or both (Figure 4).

On first glance these observations seem contradictory. The extreme block of replication at *rrnH* in *oriC*$^+$ *oriZ*$^+$ *ΔrecB* cells suggests that the role of RecBCD is extremely important, while in the absence of Rep at least some forks are able to proceed. On the other hand, *ΔrecB* cells do not show an extension of the time taken to duplicate the chromosome [29], in contrast to cells lacking Rep helicase [19,23,29], suggesting that the maintenance of rapid genome duplication is far more dependent on Rep helicase than RecBCD, as suggested [29]. Our data support the idea that the key may be the state of the replisome at sites of conflict, as suggested [29]. Replication appears to be able to proceed without much difficulty in *ΔrecB* cells until very highly-transcribed regions are reached in an orientation opposite to normal. As the overall co-directionality of replication and transcription is only just over 50% in *E. coli* [56], replication forks both coming from *oriC* and the

ectopic origins *oriZ* and *oriX* will encounter several genes in an orientation opposite to normal and there is no indication that these conflicts stop progression of replication. It seems that the presence of Rep helicase is fully sufficient to facilitate progression of replisomes through these areas. Forks encountering an *rrn* operon in an orientation opposite to normal apparently trigger a very different situation. It was shown before that in *ΔuvrD Δrep rpo** cells both RecBCD and RecA are essential for survival, suggesting that not only the degradation of DNA by RecBCD but also the loading of RecA is required for the continuation of DNA replication [29]. Our data suggest that the reason for this is at least twofold. The replication profiles reveal that at such replication-transcription conflicts an intermediate is generated that is accessible to degradation by SbcCD (Figure 7) and other nucleases such as RecJ [14]. Thus, one reason for the inability to restart replication in the absence of RecBCD appears to be that replication fork structures are extensively resected. There are few signs of degradation in *Δrep* cells, suggesting that it either does not take place or is much more limited (Figure 6). However, even in the absence of SbcCD the *rrnH* operon still forms a hard stop to DNA replication in *ΔrecB* cells, in line with the idea that without the ability to load RecA via RecBCD replication cannot continue [29].

Our data are in line with the idea that RecBCD is required at sites where the block to replication forks is severe. A brief pause of replisome progression without the disassembly of the components is unlikely to require processing by RecBCD, and with the replisome intact it is unlikely that RecBCD will be able to access replication fork structures [29,57]. The action of accessory helicases such as Rep and UvrD is likely to be sufficient to allow replication to proceed. In contrast, a prolonged block to the progression of synthesis increases the likelihood of replisomes being inactivated and eventually disassembled [58–60]. Once the fork is disassembled the mere action of accessory helicases will be insufficient to restart synthesis. In addition, the disassembly of the replisome will also make the replication fork intermediates accessible for other enzymes such as nucleases. Indeed we have reported before that nascent DNA is extensively degraded via RecJ and RecBCD at sites where replication was stalled at UV-induced lesions if restart of synthesis is artificially prevented [61]. Thus, in the absence of RecBCD replication will be able to proceed at most sites where replication-transcription conflicts occur, but if the clashes cause a prolonged delay of replication with a partial or full disassembly of replisomes, cells struggle rather significantly with the restart of replication, thereby exposing replication intermediates to the action of exonucleases such as SbcCD and RecJ over extended periods of time (Figure 7) [14,61].

But what is causing the degradation in the termination area of *ΔrecB* cells? The involvement of SbcCD, which has been shown to cleave hairpin secondary structures in DNA close to the unpaired tip [62,63], has led to the suggestion that as part of termination replisomes move past each other, thereby transiently over-replicating a section of the chromosome. The over-replicated stretch might be incised by SbcCD, which would explain the degradation observed [35]. However, this hypothesis is unable to explain the existing data. Our replication profiles show that even in the absence of SbcCD degradation is still taking place, but the extent is much more limited (Figure 1), in line with the replication profiles of *ΔrecB ΔxonA ΔsbcCD* cells (Figure 1) [35,36]. Thus, it appears that the event that enables degradation via SbcCD in *ΔrecB* cells is not prevented in the

absence of ExoI or by SbcCD, but the degradation following this event is far less extensive. Furthermore, the replication profiles of *ΔrecB* cells with the chromosome linearized in the +200 kb position demonstrate that extensive amounts of degradation are still taking place despite the fact that the two replisomes can never move past each other (Figure 2).

In two recent studies Sinha and colleagues thoroughly analysed the degradation in the termination area [34,36]. Their results suggest that the degradation is at least in part triggered by septum closure. Furthermore, it was shown that, following the initiating event, one daughter cell is generated that had lost sequences of the terminus region and will not generate a viable daughter cell again, while the second daughter cell had retained what appeared to be a complete terminus region. The latter cell generated again one cell in which sequences of the terminus region are lost and a second cell retaining the terminus region [34,36], suggesting that the initiating event results in a defect that is retained in the surviving cell. They proposed a model in which a broken replication fork near the terminus region triggers a broken, linear copy of a chromosome to be segregated into one daughter cell. The broken fork leads to a form of replication that has some similarity to rolling-circle replication, retaining one circular chromosome in one cell and generating again a linear chromosome which is segregated into the daughter cell [34,36]. Their model not only explains the pattern of one non-viable and one viable cell, the latter of which generates again a non-viable and a viable cell, but it also predicts that linearization of the chromosome should result in the degradation of one end, while the other end should be protected, as observed in cells where the chromosome is linearized near *dif* [34,36] (Figure 2).

In contrast to the model proposed by Wendel and co-workers, the model proposed by Sinha and colleagues predicts that the initiating event in *ΔrecB* cells is independent of SbcCD, which fits well with our own observation that the loss of marker frequency near *dif* in *ΔrecB ΔsbcCD* cells is essentially as extreme as in *ΔrecB* cells while only the extent of degradation is reduced (Figure 1). Both a broken replication fork and the subsequent guillotining of the chromosome by septation would lead to marker loss, but the lack of degradation would cause the resulting valley of the replication profile to be much narrower. In principle this idea fits well with our data. While in double origin cells degradation is observed both in the termination area and at sites of replication-transcription conflicts (Figure 4), degradation in both areas appears to be of a different nature. The degradation at sites of replication-transcription conflicts is less extreme than the degradation in the termination area, where a substantial depletion of terminus area sequences takes place. The data are in line with the idea that at sites of replication-transcription conflicts nascent DNA is resected by nucleases such as SbcCD and RecJ (Figure 7) [14], similar to a situation where the restart of forks at small DNA lesions blocking progression of the replicative polymerase is prevented [61]. As in this case the parental strands are retained, degradation is only moderate, but if it proceeds far enough it can still interfere with the activity of the ectopic replication origin, explaining why origin firing of the ectopic origins is so much reduced as long as SbcCD is present (Figure 4). However, chromosome breakage by a broken replication fork or guillotining of the chromosome will cause more degradation due to the loss of the parental strands, as demonstrated by the disappearance of the fluorescence signal in the termination area [34,36]. As origin-

proximal areas are segregated early, breakage would be unlikely to occur here, as they would have been moved out of the area where septation occurs.

The data presented by Sinha and colleagues suggest that the degradation in the termination area is not directly linked to the fusion of replication forks [34,36]. Indeed, all of our replication profiles of *ΔrecB* cells show a remarkable consistency of the location of the low point in the termination area, even though the replichore arrangements are quite seriously distorted in *oriC*$^+$ *oriX*$^+$ and *oriC*$^+$ *oriZ*$^+$ cells (cf. Figure 4 and Suppl. Figure 2). In addition, if degradation was purely related to the fusion of forks, degradation both in the native and the ectopic termination areas should be similar, which, as just discussed, they are not. So has the fusion of two forks got nothing to do with the degradation? One argument against this notion is our observation that degradation in cells in which the chromosome is linearized 200 kb from *dif* is not only present in both chromosomal ends, but the low point is also significantly shifted. In fact, the model proposed by Sinha and colleagues would predict that degradation of one chromosome end should be protected, identical to the situation in cells where the chromosome is linearized near *dif*. So what causes this distinct difference? We cannot rule out that the symmetrical degradation is triggered by a secondary event that only happens if the chromosome is linearized within the +200 kb region. However, given that degradation is symmetrical in all *ΔrecB* constructs with the exception of cells where the chromosome linearized near *dif*, we prefer the explanation that the initiation of degradation is similar in all cells. Cells in which the chromosome is linearized near *dif* are an exception in which one chromosome end is protected from degradation. The fact that an *rpo** mutation allowed more SbcCD-dependent degradation to occur but did not alter the extent of degradation in *ΔrecB ΔsbcCD* cells (Figure 3) supports the idea that stable protein-DNA complexes will slow degradation. However, we do not know what is responsible for this protection. It is not caused by proximity of a *ter*/Tus complex to the linearization site, as the deletion of *tus* had no impact on the protection of the non-degraded chromosome arm (Figure 2).

But if the mechanism of degradation in *ΔrecB* cells in which the chromosome is linearized at +200 kb is the same as in *ΔrecB* single mutants, what is causing the degradation? Our data support the idea that forks stalled for prolonged periods at sites of replication-transcription conflicts might get disassembled, thereby allowing nucleases to gain access and start resection of nascent DNA (Figure 7). However, the model by Sinha and colleagues [34,36] suggests a second and completely independent event, a broken replication fork, to trigger degradation, which is also mediated by SbcCD (Figure 1). This then is exacerbated by guillotining of the chromosome. This model not only struggles to explain the symmetrical degradation in our *ΔrecB* cells where the chromosome is linearized at +200 kb, but it also struggles to explain why over-replication of the termination area is observed in *ΔrecD* single mutants [45]. Since two-ended dsDNA breaks are not repaired efficiently in the absence of RecD [64], the absence of RecD should still result in at least some depletion of sequences at break sites. Instead, over-replication is observed in the termination area of *ΔrecD* cells [45].

Could there be a different scenario? If disassembled replisomes require RecBCD for the efficient restart of replication and otherwise trigger degradation via nucleases such as SbcCD, could it not be that in an analogous way replisomes disassemble in the termination area, thereby

triggering nuclease degradation in the absence of RecBCD? Forks certainly will disassemble as part of the normal termination process, which might lead to intermediates accessible to nucleases in a fraction of cells [34,36], but other factors, such as the accumulation of torsional stress, could lead to some pausing of synthesis as replication is close to being completed [65]. The resulting degradation would initially be a resection similar to that observed at *rrnH* in *oriC*$^+$ *oriZ*$^+$ *ΔrecB* cells, which would be relatively mild. This is in line with the observation that degradation in *ΔrecB ftsA(ts)* cells, in which septum closure is inhibited, is mild at restrictive temperature [34]. However, any degradation will interfere with successful chromosome segregation, as degradation would interfere with completion of chromosome duplication. The inability to fully segregate the chromosomes would then easily explain why guillotining is taking place, as suggested [34,36]. As the initiating event is not a dsDNA break, lack of RecD would not have as much of an impact. Given that *ΔrecD* cells show a hyper-recombination phenotype [66], stalled forks might trigger more recombination events which would potentially allow completion of DNA replication. This would prevent any guillotining, while the elevated recombination frequency would explain the observed over-replication [45]. In addition, this scenario has fewer difficulties explaining why degradation is taking place at both chromosome ends in *ΔrecB* cells in which the chromosome is linearized at +200 kb. It would predict that some degradation would indeed be dependent on the location of fork fusion, but that the excessive loss of sequences of the termination area is triggered by septum closure. Indeed, a connection is formed between the FtsZ-ring and the Ter macrodomain [67], which might explain why the location of the low point of the replication profiles in *ΔrecB* cells is so similar in a variety of different backgrounds (cf. Figures 1, 4 and Suppl. Figure 2) unless chromosome positioning is disturbed in cells lacking FtsK translocase [34].

While the above order of events might be better suited to explain some of the experimental data, they struggle to explain the persistent degradation observed by Sinha and colleagues. The pattern observed suggests that one chromosomal copy is degraded and produces a cell that is not viable, while the second copy remains intact enough to continue a full replication cycle. However, some sort of defect must remain, as the same cycle is repeated. The more or less stochastic guillotining of the chromosome, despite any positioning effects that might take place, is unlikely to affect only one chromosomal copy with such specificity. In addition, the inability to segregate chromosomes efficiently, either due to a broken replication fork or a partially under-replicated chromosome, would be expected to prevent formation of the Z-ring. Multiple proteins, including SulA, SlmA and MinC, are involved in preventing Z-ring formation over the nucleoid in *E. coli* [67] However, when we compared cell length in wild type and *ΔrecB* cells grown in LB broth, cells lacking RecB show a reduction of cell size with little indication of filamentation (Suppl. Figure 3). Thus, we believe the precise nature of the molecular events leading to the degradation of DNA in cells lacking RecB still remains to be determined.

ACCESSION NUMBERS

All relevant raw sequencing data can be accessed at the European Nucleotide Archive (http://www.ebi.ac.uk/ena/data/view/PRJEB27616)

SUPPLEMENTARY MATERIAL

Supplementary Material is available online.

FUNDING

This work was supported by Research Grants BB/K015729/1 and BB/N014995/1 from the Biotechnology and Biological Sciences Research Council to CJR.

CONFLICT OF INTEREST

The authors declare that there are no conflicts of interest.

ACKNOWLEDGEMENTS

The authors wish to thank Michelle Hawkins, Ed Bolt and Ivana Ivančić-Baće for critical reading of the manuscript.

REFERENCES

[1] L. Dewachter, N. Verstraeten, M. Fauvart, J. Michiels, An integrative view of cell cycle control in *Escherichia coli*, FEMS Microbiol. Rev. (2018). doi:10.1093/femsre/fuy005.

[2] C. Tomasetti, L. Li, B. Vogelstein, Stem cell divisions, somatic mutations, cancer etiology, and cancer prevention, Science. 355 (2017) 1330–1334. doi:10.1126/science.aaf9011.

[3] T.M. Pham, K.W. Tan, Y. Sakumura, K. Okumura, H. Maki, M.T. Akiyama, A single-molecule approach to DNA replication in *Escherichia coli* cells demonstrated that DNA polymerase III is a major determinant of fork speed, Mol. Microbiol. 90 (2013) 584–596. doi:10.1111/mmi.12386.

[4] I.G. Duggin, R.G. Wake, S.D. Bell, T.M. Hill, The replication fork trap and termination of chromosome replication, Mol. Microbiol. 70 (2008) 1323–1333. doi:10.1111/j.1365-2958.2008.06500.x.

[5] J.U. Dimude, S.L. Midgley-Smith, M. Stein, C.J. Rudolph, Replication Termination: Containing Fork Fusion-Mediated Pathologies in *Escherichia coli*, Genes. 7 (2016). doi:10.3390/genes7080040.

[6] C. Neylon, A.V. Kralicek, T.M. Hill, N.E. Dixon, Replication termination in *Escherichia coli*: structure and antihelicase activity of the Tus-*Ter* complex, Microbiol. Mol. Biol. Rev. MMBR. 69 (2005) 501–526. doi:10.1128/MMBR.69.3.501-526.2005.

[7] R. Reyes-Lamothe, E. Nicolas, D.J. Sherratt, Chromosome replication and segregation in bacteria, Annu. Rev. Genet. 46 (2012) 121–143. doi:10.1146/annurev-genet-110711-155421.

[8] P. McGlynn, N.J. Savery, M.S. Dillingham, The conflict between DNA replication and transcription, Mol. Microbiol. 85 (2012) 12–20. doi:10.1111/j.1365-2958.2012.08102.x.

[9] M.M. Cox, Recombinational DNA repair of damaged replication forks in *Escherichia coli*: questions, Annu. Rev. Genet. 35 (2001) 53–82. doi:10.1146/annurev.genet.35.102401.090016.

[10] H. Merrikh, Y. Zhang, A.D. Grossman, J.D. Wang, Replication-transcription conflicts in bacteria, Nat. Rev. Microbiol. 10 (2012) 449–458. doi:10.1038/nrmicro2800.

[11] H.Y. Wu, S.H. Shyy, J.C. Wang, L.F. Liu, Transcription generates positively and negatively supercoiled domains in the template, Cell. 53 (1988) 433–440.

[12] L. Olavarrieta, P. Hernández, D.B. Krimer, J.B. Schvartzman, DNA knotting caused by head-on collision of transcription and replication, J. Mol. Biol. 322 (2002) 1–6.

[13] D. Ivanova, T. Taylor, S.L. Smith, J.U. Dimude, A.L. Upton, M.M. Mehrjouy, O. Skovgaard, D.J. Sherratt, R. Retkute, C.J. Rudolph, Shaping the landscape of the *Escherichia coli* chromosome: replication-transcription encounters in cells with an ectopic replication origin, Nucleic Acids Res. 43 (2015) 7865–7877. doi:10.1093/nar/gkv704.

[14] A.L. De Septenville, S. Duigou, H. Boubakri, B. Michel, Replication fork reversal after replication-transcription collision, PLoS Genet. 8 (2012) e1002622. doi:10.1371/journal.pgen.1002622.

[15] A. Srivatsan, A. Tehranchi, D.M. MacAlpine, J.D. Wang, Co-Orientation of Replication and Transcription Preserves Genome Integrity, PLoS Genet. 6 (2010) e1000810. doi:10.1371/journal.pgen.1000810.

[16] J.D. Wang, M.B. Berkmen, A.D. Grossman, Genome-wide coorientation of replication and transcription reduces adverse effects on replication in *Bacillus subtilis*, Proc. Natl. Acad. Sci. U. S. A. 104 (2007) 5608–5613. doi:10.1073/pnas.0608999104.

[17] H. Boubakri, A.L. de Septenville, E. Viguera, B. Michel, The helicases DinG, Rep and UvrD cooperate to promote replication across transcription units *in vivo*, EMBO J. 29 (2010) 145–157. doi:10.1038/emboj.2009.308.

[18] H. Merrikh, C. Machón, W.H. Grainger, A.D. Grossman, P. Soultanas, Co-directional replication-transcription conflicts lead to replication restart, Nature. 470 (2011) 554–557. doi:10.1038/nature09758.

[19] J. Atkinson, M.K. Gupta, C.J. Rudolph, H. Bell, R.G. Lloyd, P. McGlynn, Localization of an accessory helicase at the replisome is critical in sustaining efficient genome duplication, Nucleic Acids Res. 39 (2011) 949–957. doi:10.1093/nar/gkq889.

[20] C.P. Guy, J. Atkinson, M.K. Gupta, A.A. Mahdi, E.J. Gwynn, C.J. Rudolph, P.B. Moon, I.C. van Knippenberg, C.J. Cadman, M.S. Dillingham, R.G. Lloyd, P. McGlynn, Rep provides a second motor at the replisome to promote duplication of protein-bound DNA, Mol. Cell. 36 (2009) 654–666. doi:10.1016/j.molcel.2009.11.009.

[21] J.-G. Brüning, J.L. Howard, P. McGlynn, Accessory replicative helicases and the replication of protein-bound DNA, J. Mol. Biol. 426 (2014) 3917–3928. doi:10.1016/j.jmb.2014.10.001.

[22] M.L. Bochman, N. Sabouri, V.A. Zakian, Unwinding the functions of the Pif1 family helicases, DNA Repair. 9 (2010) 237–249. doi:10.1016/j.dnarep.2010.01.008.

[23] H.E. Lane, D.T. Denhardt, The rep mutation. IV. Slower movement of replication forks in *Escherichia coli rep* strains, J. Mol. Biol. 97 (1975) 99–112.

[24] M.S. Dillingham, S.C. Kowalczykowski, RecBCD enzyme and the repair of double-stranded DNA breaks, Microbiol. Mol. Biol. Rev. MMBR. 72 (2008) 642–671, Table of Contents. doi:10.1128/MMBR.00020-08.

[25] B. Michel, A.K. Sinha, D.R.F. Leach, Replication Fork Breakage and Restart in *Escherichia coli*, Microbiol. Mol. Biol. Rev. MMBR. 82 (2018). doi:10.1128/MMBR.00013-18.

[26] J. Wiktor, M. van der Does, L. Büller, D.J. Sherratt, C. Dekker, Direct observation of end resection by RecBCD during double-stranded DNA break repair *in vivo*, Nucleic Acids Res. 46 (2018) 1821–1833. doi:10.1093/nar/gkx1290.

[27] G.R. Smith, How RecBCD enzyme and Chi promote DNA break repair and recombination: a molecular biologist's view, Microbiol. Mol. Biol. Rev. MMBR. 76 (2012) 217–228. doi:10.1128/MMBR.05026-11.

[28] M.R. Singleton, M.S. Dillingham, M. Gaudier, S.C. Kowalczykowski, D.B. Wigley, Crystal structure of RecBCD enzyme reveals a machine for processing DNA breaks, Nature. 432 (2004) 187–193. doi:10.1038/nature02988.

[29] A.H. Syeda, J. Atkinson, R.G. Lloyd, P. McGlynn, The Balance between Recombination Enzymes and Accessory Replicative Helicases in Facilitating Genome Duplication, Genes. 7 (2016) 42. doi:10.3390/genes7080042.

[30] M. Uzest, S.D. Ehrlich, B. Michel, Lethality of *rep recB* and *rep recC* double mutants of *Escherichia coli*, Mol. Microbiol. 17 (1995) 1177–1188.

[31] B. Michel, S.D. Ehrlich, M. Uzest, DNA double-strand breaks caused by replication arrest, EMBO J. 16 (1997) 430–438.

[32] K.J. Kuong, A. Kuzminov, Disintegration of nascent replication bubbles during thymine starvation triggers RecA- and RecBCD-dependent replication origin destruction, J. Biol. Chem. 287 (2012) 23958–23970. doi:10.1074/jbc.M112.359687.

[33] C.J. Rudolph, A.L. Upton, A. Stockum, C.A. Nieduszynski, R.G. Lloyd, Avoiding chromosome pathology when replication forks collide, Nature. 500 (2013) 608–611. doi:10.1038/nature12312.

[34] A.K. Sinha, A. Durand, J.-M. Desfontaines, I. Iurchenko, H. Auger, D.R.F. Leach, F.-X. Barre, B. Michel, Division-induced DNA double strand breaks in the chromosome terminus region of *Escherichia coli* lacking RecBCD DNA repair enzyme, PLoS Genet. 13 (2017) e1006895. doi:10.1371/journal.pgen.1006895.

[35] B.M. Wendel, J.M. Cole, C.T. Courcelle, J. Courcelle, SbcC-SbcD and ExoI process convergent forks to complete chromosome replication, Proc. Natl. Acad. Sci. U. S. A. 115 (2018) 349–354. doi:10.1073/pnas.1715960114.

[36] A.K. Sinha, C. Possoz, A. Durand, J.-M. Desfontaines, F.-X. Barre, D.R.F. Leach, B. Michel, Broken replication forks trigger heritable DNA breaks in the terminus of a circular chromosome, PLOS Genet. 14 (2018) e1007256. doi:10.1371/journal.pgen.1007256.

[37] L.C. Thomason, N. Costantino, D.L. Court, *E. coli* genome manipulation by P1 transduction, Curr. Protoc. Mol. Biol. Ed. Frederick M Ausubel Al. Chapter 1 (2007) Unit 1.17. doi:10.1002/0471142727.mb0117s79.

[38] K.A. Datsenko, B.L. Wanner, One-step inactivation of chromosomal genes in *Escherichia coli* K-12 using PCR products, Proc. Natl. Acad. Sci. U. S. A. 97 (2000) 6640–6645. doi:10.1073/pnas.120163297.

[39] T.G. Bernhardt, P.A.J. de Boer, The *Escherichia coli* amidase AmiC is a periplasmic septal ring component exported via the twin-arginine transport pathway, Mol. Microbiol. 48 (2003) 1171–1182.

673 [40] A.A. Mahdi, C. Buckman, L. Harris, R.G. Lloyd, Rep and PriA helicase activities prevent RecA from provoking
674 unnecessary recombination during replication fork repair, Genes Dev. 20 (2006) 2135–2147.
675 doi:10.1101/gad.382306.

676 [41] T. Cui, N. Moro-oka, K. Ohsumi, K. Kodama, T. Ohshima, N. Ogasawara, H. Mori, B. Wanner, H. Niki, T.
677 Horiuchi, *Escherichia coli* with a linear genome, EMBO Rep. 8 (2007) 181–187. doi:10.1038/sj.embor.7400880.

678 [42] E.A. Kouzminova, A. Kuzminov, Chromosome demise in the wake of ligase-deficient replication, Mol. Microbiol.
679 84 (2012) 1079–1096. doi:10.1111/j.1365-2958.2012.08076.x.

680 [43] R.G. Lloyd, C. Buckman, Identification and genetic analysis of sbcC mutations in commonly used *recBC sbcB*
681 strains of *Escherichia coli* K-12, J. Bacteriol. 164 (1985) 836–844.

682 [44] F.P. Gibson, D.R. Leach, R.G. Lloyd, Identification of *sbcD* mutations as cosuppressors of *recBC* that allow
683 propagation of DNA palindromes in *Escherichia coli* K-12., J. Bacteriol. 174 (1992) 1222–1228.
684 doi:10.1128/jb.174.4.1222-1228.1992.

685 [45] B.M. Wendel, C.T. Courcelle, J. Courcelle, Completion of DNA replication in *Escherichia coli*, Proc. Natl. Acad.
686 Sci. U. S. A. 111 (2014) 16454–16459. doi:10.1073/pnas.1415025111.

687 [46] J.U. Dimude, A. Stockum, S.L. Midgley-Smith, A.L. Upton, H.A. Foster, A. Khan, N.J. Saunders, R. Retkute, C.J.
688 Rudolph, The Consequences of Replicating in the Wrong Orientation: Bacterial Chromosome Duplication
689 without an Active Replication Origin, MBio. 6 (2015). doi:10.1128/mBio.01294-15.

690 [47] G. Bokinsky, E.E.K. Baidoo, S. Akella, H. Burd, D. Weaver, J. Alonso-Gutierrez, H. García-Martín, T.S. Lee, J.D.
691 Keasling, HipA-triggered growth arrest and β-lactam tolerance in *Escherichia coli* are mediated by RelA-
692 dependent ppGpp synthesis, J. Bacteriol. 195 (2013) 3173–3182. doi:10.1128/JB.02210-12.

693 [48] S.B. Korch, T.M. Hill, Ectopic Overexpression of Wild-Type and Mutant *hipA* Genes in *Escherichia coli*: Effects
694 on Macromolecular Synthesis and Persister Formation, J. Bacteriol. 188 (2006) 3826–3836.
695 doi:10.1128/JB.01740-05.

696 [49] M. Cashel, D. Gentry, V. Hernandez, D. Vinella, The stringent response in *Escherichia coli* and *Salmonella*
697 *typhimurium*, in: *Esherichia Coli* Salmonella Cell. Mol. Biol., Second Edition, ASM Press, Washington DC, n.d.:
698 pp. 1458–1496.

699 [50] B.J. Paul, M.M. Barker, W. Ross, D.A. Schneider, C. Webb, J.W. Foster, R.L. Gourse, DksA: a critical component
700 of the transcription initiation machinery that potentiates the regulation of rRNA promoters by ppGpp and the
701 initiating NTP, Cell. 118 (2004) 311–322. doi:10.1016/j.cell.2004.07.009.

702 [51] D.S. Black, A.J. Kelly, M.J. Mardis, H.S. Moyed, Structure and organization of hip, an operon that affects lethality
703 due to inhibition of peptidoglycan or DNA synthesis, J. Bacteriol. 173 (1991) 5732–5739.

704 [52] D.S. Black, B. Irwin, H.S. Moyed, Autoregulation of hip, an operon that affects lethality due to inhibition of
705 peptidoglycan or DNA synthesis, J. Bacteriol. 176 (1994) 4081–4091.

706 [53] C.J. Rudolph, P. Dhillon, T. Moore, R.G. Lloyd, Avoiding and resolving conflicts between DNA replication and
707 transcription, DNA Repair. 6 (2007) 981–993. doi:10.1016/j.dnarep.2007.02.017.

708 [54] B.W. Trautinger, R.P. Jaktaji, E. Rusakova, R.G. Lloyd, RNA polymerase modulators and DNA repair activities
709 resolve conflicts between DNA replication and transcription, Mol. Cell. 19 (2005) 247–258.
710 doi:10.1016/j.molcel.2005.06.004.

711 [55] X. Wang, C. Lesterlin, R. Reyes-Lamothe, G. Ball, D.J. Sherratt, Replication and segregation of an *Escherichia*
712 *coli* chromosome with two replication origins, Proc. Natl. Acad. Sci. U. S. A. 108 (2011) E243-250.
713 doi:10.1073/pnas.1100874108.

714 [56] M.J. McLean, K.H. Wolfe, K.M. Devine, Base composition skews, replication orientation, and gene orientation in
715 12 prokaryote genomes, J. Mol. Evol. 47 (1998) 691–696.

716 [57] A.H. Syeda, M. Hawkins, P. McGlynn, Recombination and replication, Cold Spring Harb. Perspect. Biol. 6 (2014)
717 a016550. doi:10.1101/cshperspect.a016550.

718 [58] K.A. Mettrick, I. Grainge, Stability of blocked replication forks *in vivo*, Nucleic Acids Res. 44 (2016) 657–668.
719 doi:10.1093/nar/gkv1079.

720 [59] K.J. Marians, H. Hiasa, D.R. Kim, C.S. McHenry, Role of the Core DNA Polymerase III Subunits at the
721 Replication Fork α IS THE ONLY SUBUNIT REQUIRED FOR PROCESSIVE REPLICATION, J. Biol. Chem. 273
722 (1998) 2452–2457. doi:10.1074/jbc.273.4.2452.

723 [60] P. McGlynn, C.P. Guy, Replication forks blocked by protein-DNA complexes have limited stability *in vitro*, J.
724 Mol. Biol. 381 (2008) 249–255. doi:10.1016/j.jmb.2008.05.053.

725 [61] C.J. Rudolph, A.L. Upton, R.G. Lloyd, Maintaining replication fork integrity in UV-irradiated *Escherichia coli*
726 cells, DNA Repair. 7 (2008) 1589–1602. doi:10.1016/j.dnarep.2008.06.012.

727 [62] S.T. Lovett, The DNA exonucleases of *Escherichia coli*, EcoSal Plus. 4 (2011). doi:10.1128/ecosalplus.4.4.7.

[63] J.C. Connelly, L.A. Kirkham, D.R. Leach, The SbcCD nuclease of *Escherichia coli* is a structural maintenance of chromosomes (SMC) family protein that cleaves hairpin DNA, Proc. Natl. Acad. Sci. U. S. A. 95 (1998) 7969–7974.

[64] M.A. White, B. Azeroglu, M.A. Lopez-Vernaza, A.M.M. Hasan, D.R.F. Leach, RecBCD coordinates repair of two ends at a DNA double-strand break, preventing aberrant chromosome amplification, Nucleic Acids Res. (2018). doi:10.1093/nar/gky463.

[65] J. Gowrishankar, End of the Beginning: Elongation and Termination Features of Alternative Modes of Chromosomal Replication Initiation in Bacteria, PLoS Genet. 11 (2015) e1004909. doi:10.1371/journal.pgen.1004909.

[66] S.T. Lovett, C. Luisi-DeLuca, R.D. Kolodner, The genetic dependence of recombination in *recD* mutants of *Escherichia coli*, Genetics. 120 (1988) 37–45.

[67] J. Männik, M.W. Bailey, Spatial coordination between chromosomes and cell division proteins in *Escherichia coli*, Front. Microbiol. 6 (2015). doi:10.3389/fmicb.2015.00306.

FIGURE LEGENDS

Figure 1. The absence of nucleases modulates the extent of the marker frequency loss in the terminus area of *ΔrecB* cells. Exonucleases I, VII, SbcCD and RecJ are encoded by *xonA*, *xseA*, *sbcCD* and *recJ*, respectively. The replication profiles are generated by plotting the number of sequence reads (normalised against reads for a stationary phase wild type control) against their chromosomal location. The schematic representation of the *E. coli* chromosome above each panel shows the positions of *oriC* and *ter* sites (above) as well as the *dif* chromosome dimer resolution site and *rrn* operons *A–E, G* and *H* (below). The strains used were JD1269 (*ΔrecB*), JD1148 (*ΔrecB ΔxonA*), JD1150 (*ΔrecB ΔxseA*), JD1146 (*ΔrecB ΔsbcCD*), JD1147 (*ΔrecB ΔxonA ΔsbcCD*) and JD1139 (*ΔrecB ΔrecJ*).

Figure 2. The effect of chromosome linearization on the marker frequency loss in the terminus area of *ΔrecB* cells is dependent on the precise linearization location. The replication profiles are generated by plotting the number of sequence reads (normalised against reads for a stationary phase wild type control) against their chromosomal location. The schematic representation of the *E. coli* chromosome above each panel shows the positions of *oriC* and *ter* sites (above) as well as the *dif* chromosome dimer resolution site and *rrn* operons *A–E, G* and *H* (below). The linearization locations are shown in orange. The strains used were MG1655, JD1269 (*ΔrecB*), SLM1093 (*ΔrecB tos*), SLM1103 (*ΔrecB* N15 lysogen), SLM1100 (*ΔrecB tos* N15 lysogen), JD1306 (*ΔrecB Δtus tos +200 kb* N15 lysogen), JD1367 (*ΔrecB Δtus tos*) and JD1371 (*ΔrecB Δtus tos* N15 lysogen).

Figure 3. Modulation of RNA polymerase increases marker frequency loss in the terminus area of *ΔrecB* cells. The replication profiles are generated by plotting the number of sequence reads (normalised against reads for a stationary phase wild type control) against their chromosomal location. The schematic representation of the *E. coli* chromosome above each panel shows the positions of *oriC* and *ter* sites (above) as well as the *dif* chromosome dimer resolution site and *rrn* operons *A–E, G* and *H* (below). The strains used were MG1655, JD1269 (*ΔrecB*), JD1301 (*ΔhipA ΔrecB*), JD1294 (*ΔhipB ΔrecB*), JD1143 (*ΔrecB rpoB*35*) and JD1422 (*ΔrecB rpoB*35 ΔsbcCD*).

Figure 4. Activity of an ectopic replication origin is reduced in the absence of RecBCD due to replication-transcription conflicts. The replication profiles are generated by plotting the number of sequence reads (normalised against reads for a stationary phase wild type control) against their chromosomal location. The schematic representation of the *E. coli* chromosome above each panel shows the positions of the two origins, *oriC* and *oriZ,* and *ter* sites (above) as well as the *dif* chromosome dimer resolution site and *rrn* operons *A–E, G* and *H* (below). The strains used were RCe504 (*oriC*$^+$ *oriZ*$^+$), RCe567 (*oriC*$^+$ *oriZ*$^+$ *Δtus*), JD1144 (*oriC*$^+$ *oriZ*$^+$ *ΔrecB*), JD1140 (*oriC*$^+$ *oriZ*$^+$ *Δtus ΔrecB*) and JD1145 (*oriC*$^+$ *oriZ*$^+$ *ΔrecB rpoB*35*).

Figure 5. Maintenance of viability of *oriC*$^+$ *oriZ*$^+$ and *ΔoriC oriZ*$^+$ cells in the absence of RecBCD. The plate photographs shown are of synthetic lethality assays, as described in Materials and Methods. The relevant genotype of the construct used is shown above each photograph, with the strain number in parentheses. The fraction of white colonies is shown below, with the number of white colonies/total colonies analysed in parentheses. The plasmid used was pAM375 (*recB*$^+$) (see Supplementary Information).

Figure 6. Replication dynamics and cell viability in cells with one or two active replication origins lacking Rep helicase. **A)** Replication fork progression is blocked at highly transcribed regions replicated in a direction opposite to normal in *oriC*$^+$ *oriZ*$^+$ cells lacking Rep helicase. The replication profiles are generated by plotting the number of sequence reads (normalised against reads for a stationary phase wild type control) against their chromosomal location. The schematic representation of the *E. coli* chromosome above each panel shows the positions of the two origins, *oriC* and *oriZ,* and *ter* sites (above) as well as the *dif* chromosome dimer resolution site and *rrn* operons *A–E, G* and *H* (below). The strains used were MG1655, JD1123 (*Δrep*), RCe504 (*oriC*$^+$ *oriZ*$^+$), JD1141 (*oriC*$^+$ *oriZ*$^+$ *Δrep*) and JD1142 (*oriC*$^+$ *oriZ*$^+$ *Δrep rpoB*35*). **B)** Maintenance of viability of *oriC*$^+$ *oriZ*$^+$ and *ΔoriC oriZ*$^+$ cells in the absence of Rep helicase. The plate photographs shown are of synthetic lethality assays, as described in Materials and Methods. The relevant genotype of the construct used is shown above each photograph, with the strain number in parentheses. The fraction of white colonies is shown below, with the number of white colonies/total colonies analysed in parentheses. The plasmid used was pAM403 (*rep*$^+$) (see Supplementary Information).

Figure 7. The reduced activity of an ectopic replication origin in the absence of RecBCD is caused by SbcCD. The replication profiles are generated by plotting the number of sequence reads (normalised against reads for a stationary phase wild type control) against their chromosomal location. The schematic representation of the *E. coli* chromosome above each panel shows the positions of the two origins, *oriC* and *oriZ,* and *ter* sites (above) as well as the *dif* chromosome dimer resolution site and *rrn* operons *A–E, G* and *H* (below). The strains used were JD1428 (*oriC*$^+$ *oriZ*$^+$ *ΔsbcCD*), JD1144 (*oriC*$^+$ *oriZ*$^+$ *ΔrecB*) and JD1429 (*oriC*$^+$ *oriZ*$^+$ *ΔrecB ΔsbcCD*).

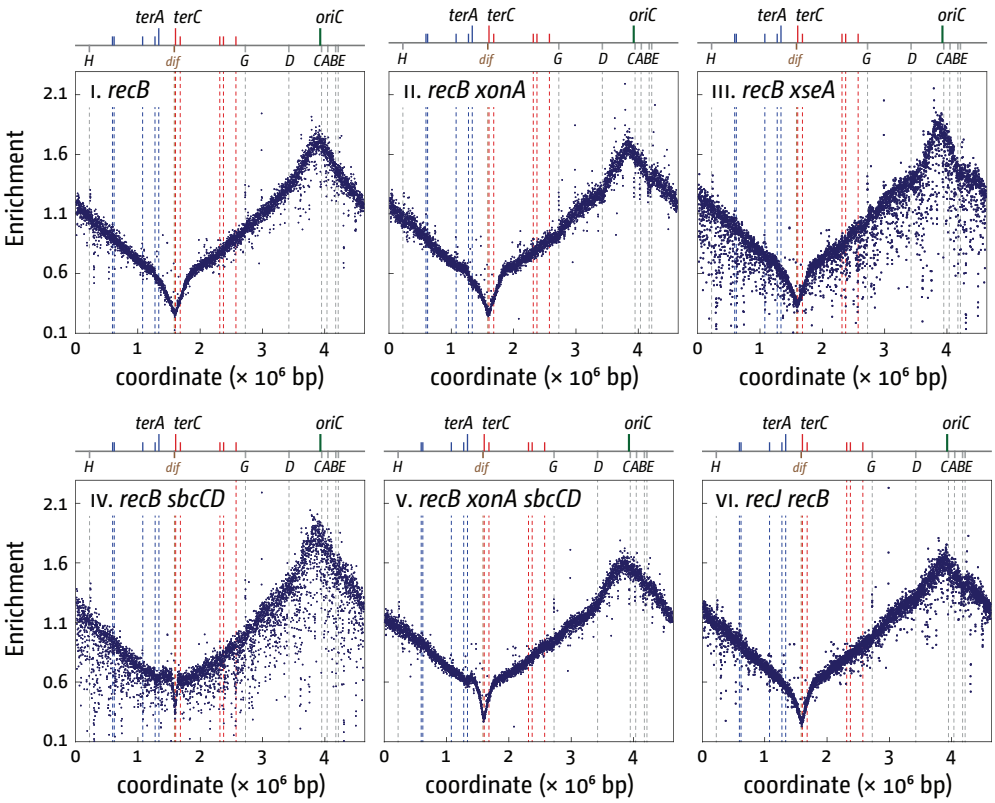
terA terC oriC
H dif G D CABE
I. recB
II. recB xonA
III. recB xseA
IV. recB sbcCD
V. recB xonA sbcCD
VI. recJ recB
Enrichment
2.1
1.6
1.1
0.6
0.1
0 1 2 3 4
coordinate (× 10⁶ bp)

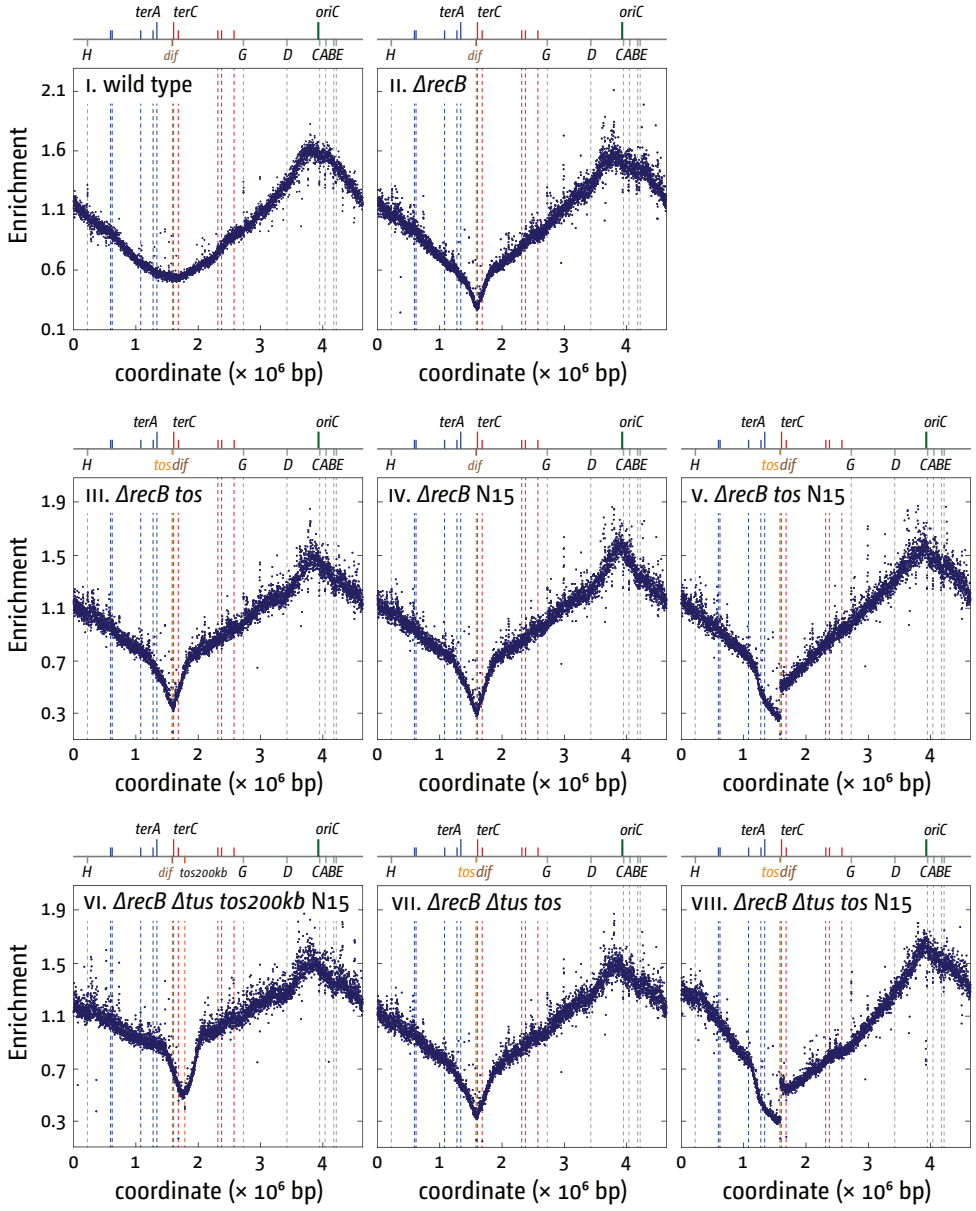
terA terC oriC
H dif G D CABE
I. wild type
II. ΔrecB
III. ΔrecB tos
IV. ΔrecB N15
V. ΔrecB tos N15
VI. ΔrecB Δtus tos200kb N15
VII. ΔrecB Δtus tos
VIII. ΔrecB Δtus tos N15
tosdif
tos200kb
Enrichment
coordinate (× 10⁶ bp)

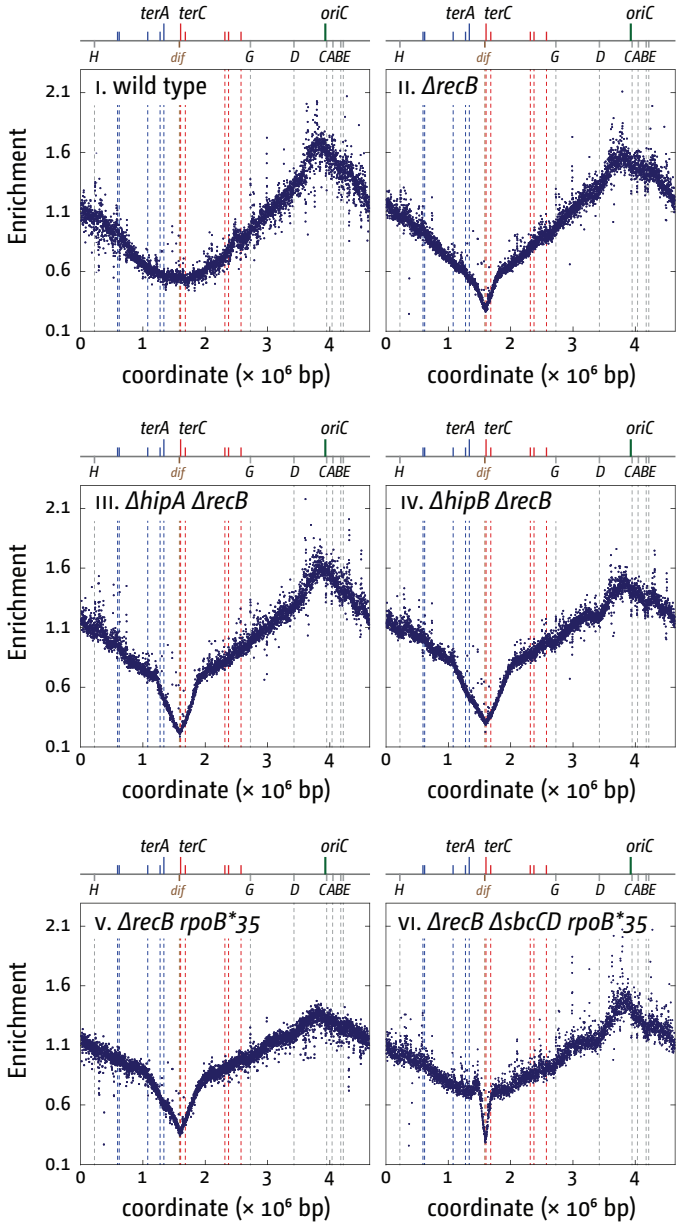
terA terC oriC
H dif G D CABE
I. wild type
II. ΔrecB
III. ΔhipA ΔrecB
IV. ΔhipB ΔrecB
V. ΔrecB rpoB*35
VI. ΔrecB ΔsbcCD rpoB*35
Enrichment
2.1
1.6
1.1
0.6
0.1
0 1 2 3 4
coordinate (× 10⁶ bp)

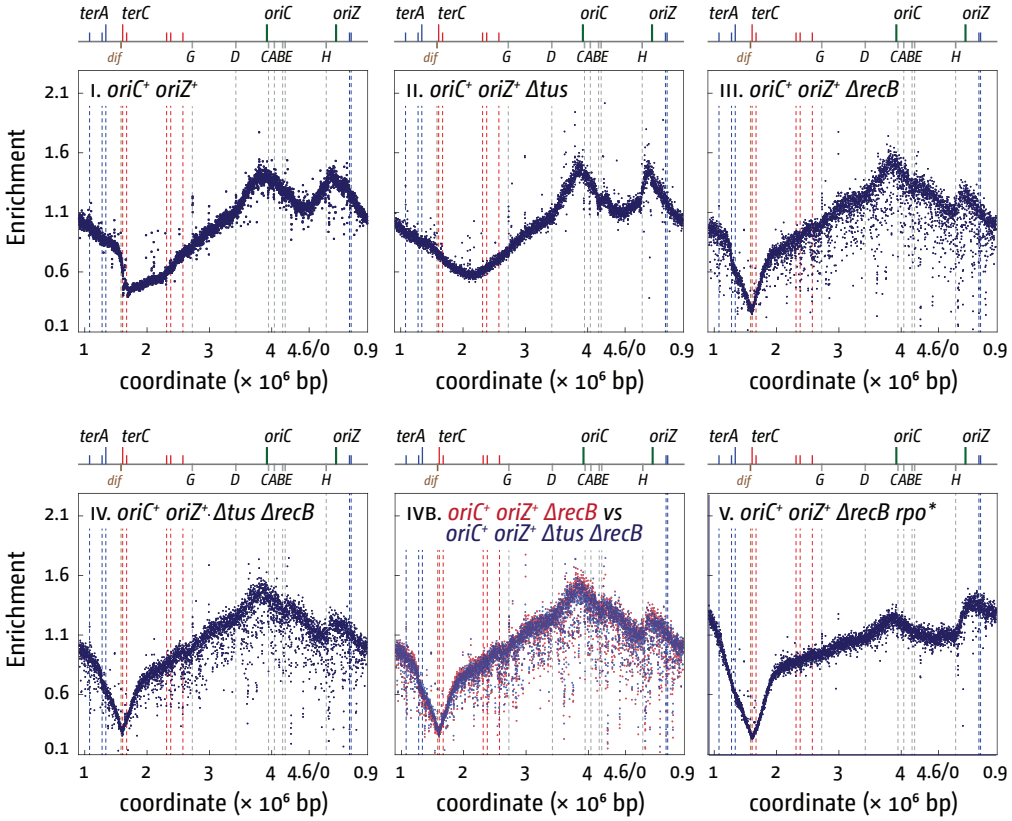
terA terC oriC oriZ
dif G D CABE H
I. oriC+ oriZ+
II. oriC+ oriZ+ Δtus
III. oriC+ oriZ+ ΔrecB
IV. oriC+ oriZ+ Δtus ΔrecB
IVB. oriC+ oriZ+ ΔrecB vs
oriC+ oriZ+ Δtus ΔrecB
V. oriC+ oriZ+ ΔrecB rpo*
Enrichment
2.1
1.6
1.1
0.6
0.1
1 2 3 4 4.6/0 0.9
coordinate (× 10⁶ bp)

I. *precB*$^{+}$/*ΔrecB*
(AU1041)

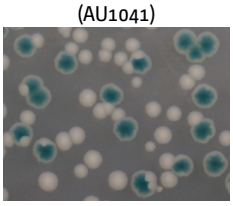

0.60 (247/409)

II. *precB*$^{+}$/*ΔrecB*
(AU1041 minimal agar)

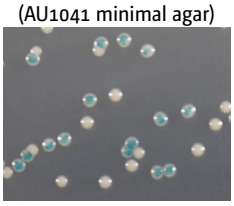

0.67 (355/532)

III. *precB*$^{+}$/*oriC*$^{+}$ *oriZ*$^{+}$
ΔrecB
(RCe601)

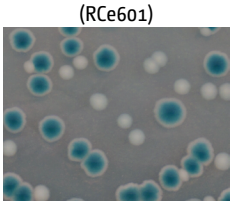

0.39 (1410/3605)

IV. *precB*$^{+}$/*oriC*$^{+}$ *oriZ*$^{+}$
ΔrecB
(RCe601 minimal agar)

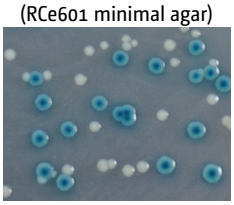

0.41 (1393/3361)

V. *precB*$^{+}$/*oriC*$^{+}$ *oriZ*$^{+}$
*ΔrecB rpoB*35*
(RCe603)

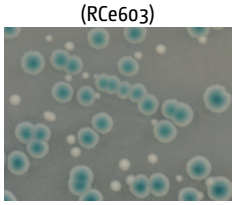

0.20 (933/4674)

VI. *precB*$^{+}$/*oriC*$^{+}$ *oriZ*$^{+}$
*ΔrecB rpoB*35*
(RCe603 minimal agar)

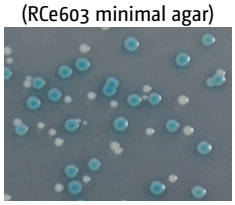

0.34 (4167/12347)

VII. *precB*$^{+}$/*oriC*$^{+}$ *oriZ*$^{+}$
ΔrecB Δtus
(JD1326)

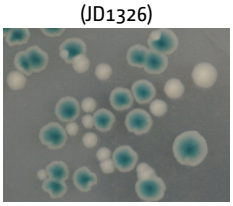

0.43 (562/1318)

VIII. *precB*$^{+}$/*oriC*$^{+}$ *oriZ*$^{+}$
ΔrecB Δtus
(JD1326 minimal agar)

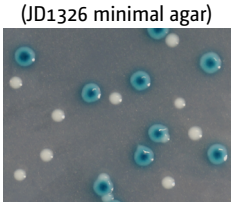

0.36 (795/2203)

IX. *precB*$^{+}$/*oriC*$^{+}$ *oriZ*$^{+}$
*ΔrecB rpoB*35 Δtus*
(JD1322)

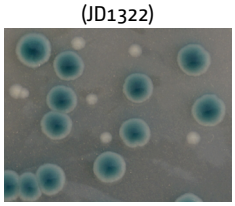

0.27 (493/1836)

X. *precB*$^{+}$/*oriC*$^{+}$ *oriZ*$^{+}$
*ΔrecB rpoB*35 Δtus*
(JD1322 minimal agar)

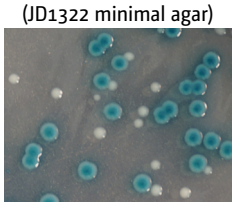

0.30 (762/2557)

XI. *precB*$^{+}$/*ΔoriC oriZ*$^{+}$
ΔrecB
(JD1101)

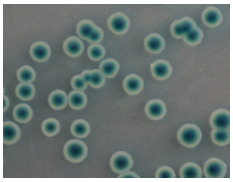

< 0.0014 (0/702)

XII. *precB*$^{+}$/*ΔoriC oriZ*$^{+}$
ΔrecB
(JD1101 minimal agar)

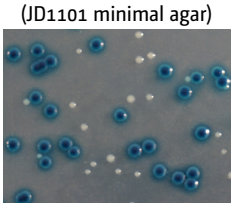

0.51 (135/262)

XIII. *precB*$^{+}$/*ΔoriC oriZ*$^{+}$
*ΔrecB rpoB*35*
(RCe613)

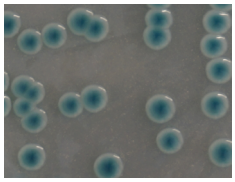

< 0.0008 (0/1184)

XIV. *precB*$^{+}$/*ΔoriC oriZ*$^{+}$
*ΔrecB rpoB*35*
(RCe613 minimal agar)

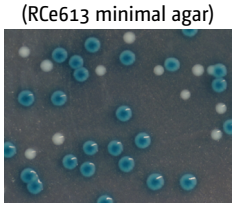

0.41 (1084/2616)

XV. *precB*$^{+}$/*ΔoriC oriZ*$^{+}$
ΔrecB Δtus
(JD1331)

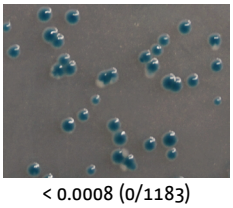

< 0.0008 (0/1183)

XVI. *precB*$^{+}$/*ΔoriC oriZ*$^{+}$
ΔrecB Δtus
(JD1331 minimal agar)

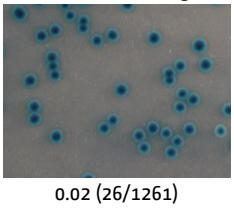

0.02 (26/1261)

XVII. *precB*$^{+}$/*ΔoriC oriZ*$^{+}$
*ΔrecB rpoB*35 Δtus*
(JD1330)

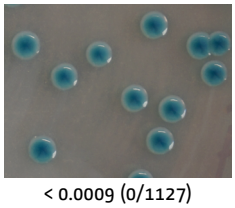

< 0.0009 (0/1127)

XVIII. *precB*$^{+}$/*ΔoriC oriZ*$^{+}$
*ΔrecB rpoB*35 Δtus*
(JD1330 minimal agar)

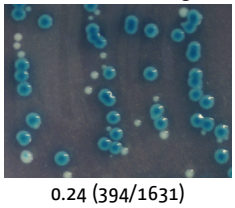

0.24 (394/1631)

A

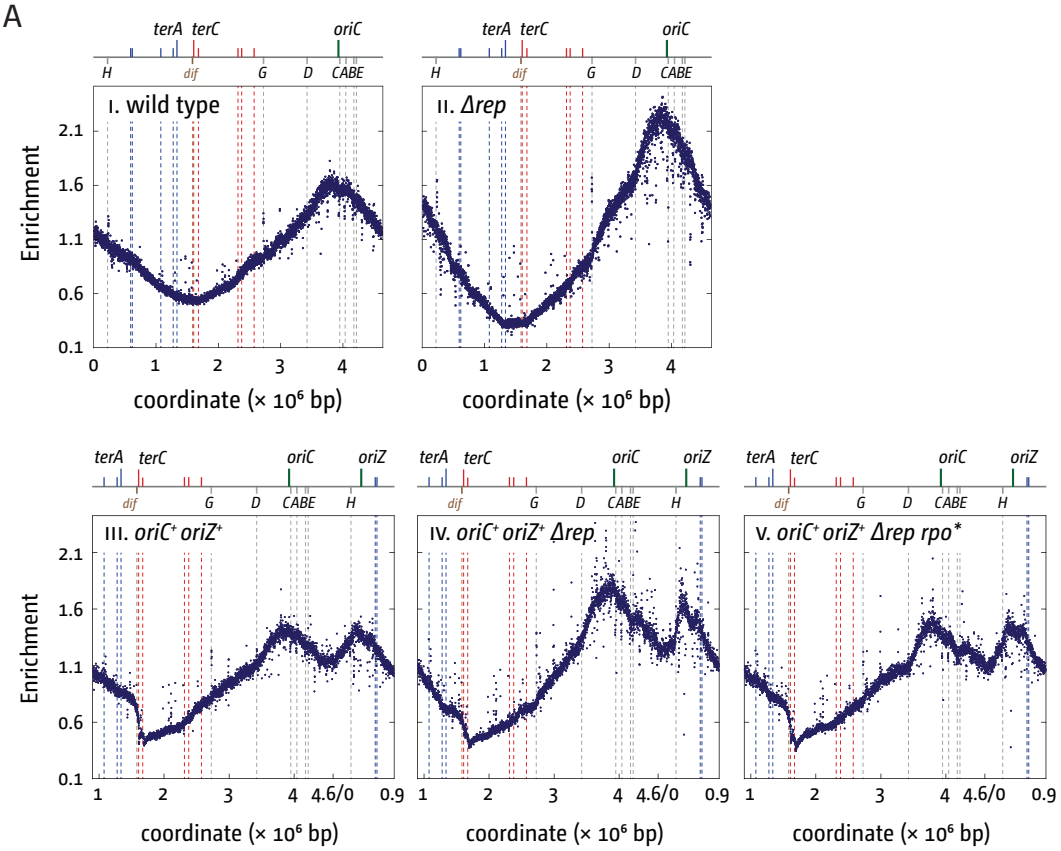
terA terC oriC
H dif G D CABE
I. wild type
II. Δrep
Enrichment
2.1
1.6
1.1
0.6
0.1
0 1 2 3 4
coordinate (× 10⁶ bp)
terA terC oriC oriZ
dif G D CABE H
III. oriC⁺ oriZ⁺
IV. oriC⁺ oriZ⁺ Δrep
V. oriC⁺ oriZ⁺ Δrep rpo*
1 2 3 4 4.6/0 0.9
coordinate (× 10⁶ bp)

B

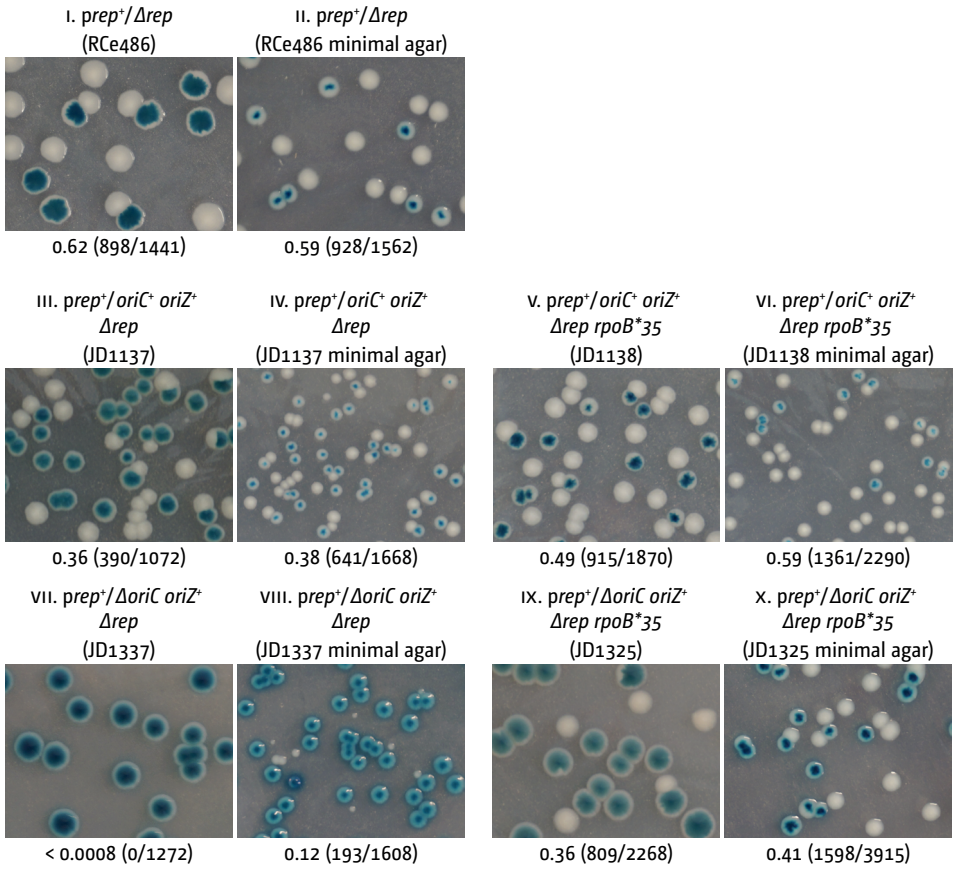
I. prep⁺/Δrep
(RCe486)
0.62 (898/1441)
II. prep⁺/Δrep
(RCe486 minimal agar)
0.59 (928/1562)
III. prep⁺/oriC⁺ oriZ⁺ Δrep
(JD1137)
0.36 (390/1072)
IV. prep⁺/oriC⁺ oriZ⁺ Δrep
(JD1137 minimal agar)
0.38 (641/1668)
V. prep⁺/oriC⁺ oriZ⁺ Δrep rpoB*35
(JD1138)
0.49 (915/1870)
VI. prep⁺/oriC⁺ oriZ⁺ Δrep rpoB*35
(JD1138 minimal agar)
0.59 (1361/2290)
VII. prep⁺/ΔoriC oriZ⁺ Δrep
(JD1337)
< 0.0008 (0/1272)
VIII. prep⁺/ΔoriC oriZ⁺ Δrep
(JD1337 minimal agar)
0.12 (193/1608)
IX. prep⁺/ΔoriC oriZ⁺ Δrep rpoB*35
(JD1325)
0.36 (809/2268)
X. prep⁺/ΔoriC oriZ⁺ Δrep rpoB*35
(JD1325 minimal agar)
0.41 (1598/3915)

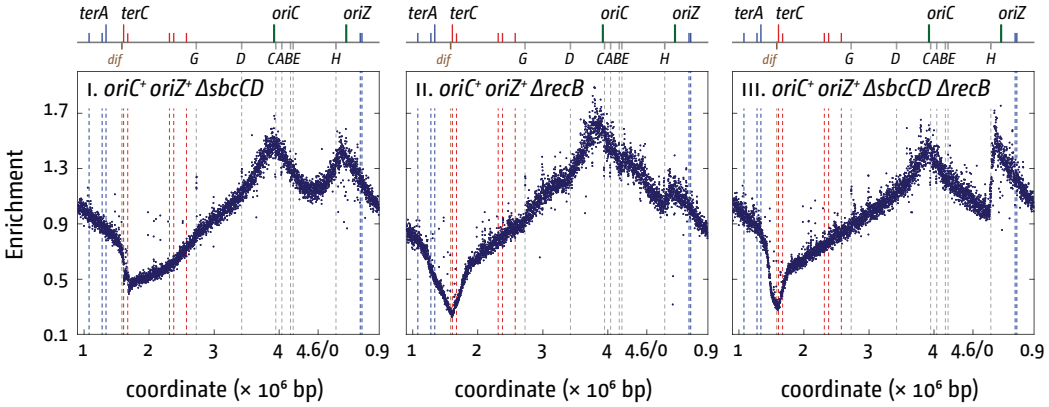
terA
terC
oriC
oriZ
dif
G
D
CABE
H
I. oriC+ oriZ+ ΔsbcCD
II. oriC+ oriZ+ ΔrecB
III. oriC+ oriZ+ ΔsbcCD ΔrecB
Enrichment
1.7
1.3
0.9
0.5
0.1
1
2
3
4
4.6/0
0.9
coordinate (× 10⁶ bp)

Supplementary Information

Replication-transcription conflicts trigger extensive DNA degradation in *Escherichia coli* cells lacking RecBCD

Juachi U. Dimude, Sarah L. Midgley-Smith and Christian J. Rudolph*

*Corresponding author: christian.rudolph@brunel.ac.uk

Division of Biosciences, College of Health and Life Sciences,
Brunel University London, Uxbridge, UB8 3PH, UK

SUPPLEMENTARY METHODS

Growth media

Luria broth (LB) and agar was modified from Luria and Burrous [1] as follows: 1% tryptone (Bacto™, BD Biosciences), 0.5% yeast extract (Bacto™, BD Biosciences) and 0.05% NaCl (Sigma Aldrich). The pH was adjusted to 7.4. Mu broth for bacteriophage P1 and N15 work contained 1% tryptone (Bacto™, BD Biosciences), 0.5% yeast extract (Bacto™, BD Biosciences) and 1% NaCl (Sigma Aldrich). The pH was adjusted to 7.4. M9 minimal medium (Sigma-Aldrich) contained 15 g/L KH2PO4, 64 g/L Na2HPO4, 2.5 g/l NaCl and 5.0 g/L NH4Cl. Before use, MgSO4, CaCl2 and glucose were added from sterile-filtered stock solutions to final concentrations of 2 mM, 0.1 mM and 0.2%, respectively, according to the manufacturer's recommendation. Doubling times of MG1655 in our growth media were 19.3 ± 1.7 min in LB and 68.8 ± 6.2 min in M9 glucose.

Marker frequency analysis by deep sequencing

Marker frequency analysis by Deep Sequencing was performed as described previously [2–4] with only minor modifications. Samples from cultures of a strain grown over night in LB broth were diluted 100-fold in fresh LB broth and incubated with vigorous aeration until an A_{600} reached 0.48 at 37°C to ensure they were in exponential growth conditions. Cultures were then diluted a second time 100-fold in pre-warmed fresh broth and grown again until an A_{600} of 0.48 was reached. Samples from these exponential phase cultures were flash-frozen in liquid nitrogen at this point for subsequent DNA extraction. For wild type, incubation of the remaining culture was continued until several hours after the culture had saturated and showed no further increase in the A_{600}. A further sample (stationary phase) was frozen at this point. DNA was then extracted using the GenElute Bacterial Genomic DNA Kit (Sigma-Aldrich). Marker frequency analysis was performed using Illumina HiSeq 2500 sequencing (fast run) to measure sequence copy number. FastQC was used for a basic metric of quality control in the raw data. Bowtie2 was used to align the sequence reads to the reference. Samtools was used to calculate the enrichment of uniquely mapped sequence tags in 1 kb windows.

For presentation of the data as a marker frequency replication profile the raw read counts for each construct were divided by the average of all read counts across the entire genome to correct for the somewhat different absolute numbers of aligned reads in the various samples. The normalised read count values for each exponentially growing sample were then divided by the corresponding normalised read count value from a stationary (non-replicating) sample. This division "cleans" the raw data significantly, because data points which are outliers caused by technical aspects (precise sequence environment interfering with library preparation or similar issues) will be similarly distorted both in the exponential and the stationary samples. However, while true in principle, we have observed that there can be variations specifically in these noisy data points even within a single batch of samples processed in parallel. If the absolute sequence reads of the genome fragments causing the noisy data points in a sample are underrepresented in comparison to the same fragments in the stationary phase sample, then the division process described above causes all of these data points to skew below the position of the neighbouring

data points. In contrast, if the absolute sequence reads of the fragments are higher than the sequence reads in the stationary control, then the same division process causes all of these data points to skew above the position of the neighbouring data points. An example of this effect can be seen in Figure 1. While the sample in panel i shows no skew, indicating that noise both in the exponential sample and the stationary sample are comparable, the samples in panels iii and iv show a clear skew of all noisy data points below the level of neighbouring data points. We do not currently know what is causing such variations even though we have run extensive tests to try to identify their cause. From our tests we suspect that a combination of factors including quality of genomic DNA preparation and library generation contributes to this effect. Whatever the reason, these problems affect mostly the noise and do not obscure the general trend of the bulk of the data points.

Bacteriophage N15 infection and lysogen preparation

For preparation of a phage N15 plate lysate, cells from an overnight culture grown in Mu were spun down and resuspended in 10 mM $MgSO_4$. Phage N15 was diluted in M9 minimal medium without glucose, 10^5–10^6 phage particles mixed with 100 µl of the prepared cells and the mixture incubated 5 min at room temperature. 2.5 ml Mu were added, followed by 2.5 ml molten Mu top agar (45°C), mixed and poured on top of a fresh Mu plate. Plates were incubated upright at 37°C for 7 h. 2 ml of M9 minimal medium without glucose were pipetted onto the plate and the top agar overlay was scraped off and transferred into a centrifugation tube. 0.5 ml chloroform was added and cell debris and top agar removed by centrifugation (10,000 rpm, 4°C). For determination of the phage N15 titer as well as infection of target strains, N15 was diluted in M9 minimal medium without glucose. 100 µl of the target or tester strain was mixed with 2.5 ml molten Mu top agar (45°C) and poured on top of a fresh Mu plate. 20 µl drops of appropriate dilutions of a lysate were placed on the top agar and incubated at room temperature until dry. The plate were then incubated over night at 37°C. For infection and lysogen preparations, 10 µl drops containing ~10^4 phage particles were used.

Plasmids used in this study

Plasmids pAM374 (*priA*$^+$), pAM375 (*recB*$^+$) and pAM403 (*rep*$^+$) have been described elsewhere [5]. All carry *lac*$^+$. pAM374 (*priA*$^+$) and pAM375 (*recB*$^+$) require IPTG for expression, as the genes are under control of the vector p*lac* promoter. pAM403 carries *rep* under control of its native promoter [5].

TABLES

Table 1: *Escherichia coli* K-12 strains

Strain number	Relevant Genotype[a]	Source
General P1 donors		
DL729	*ΔsbcCD::kan recD1009 supE supF*	David Leach
JW1500-2	BW25113 *ΔhipA728::<kan>*	CGSC [c]
JW1501	BW25113 *ΔhipB729::<kan>*	CGSC [c]
RUC1593	DY330 *pheA::oriX-cat*	Ole Skovgaard
STL2694	*xonAΔ300::cat thr-1 leuB6 proA2 supE44 kdg51 rfbD1 araC14 lacY1 galK2 xyl-5 mtl-1tsx-33 rpsL31 rac⁻*	Susan Lovett
MG1655 derivatives		
MG1655	F⁻ *rph-1*	[6]
AM1580	*ΔlacIZYA recB268::*Tn*10* pAM375	[5]
AM1675	*ΔrecB::dhfr*	A.A. Mahdi and R.G. Lloyd, unpublished
AM1775	*Δtus::cat*	[7]
AM1969	*Δrep::dhfr*	A.A. Mahdi and R.G. Lloyd, unpublished
BW66	*tos+200kb-kan*	[8]
JD1101	*ΔlacIZYA oriZ-<cat> ΔrecB::dhfr ΔoriC::kan*[b] pAM375	RCe601 A× P1.RCe395 to Km^r
JD1123	*Δrep::kan*	MG1655 × P1.N5960 to Km^r
JD1126	*ΔlacIZYA recJ284::*Tn*10*	TB28 × N4934 to Tc^r
JD1127	*ΔlacIZYA recJ284::*Tn*10* pAM375	JD1126 × pAM375 to Ap^r
JD1129	*ΔlacIZYA oriZ-<cat>* pAM403	RCe544 × pAM403 to Ap^r
JD1130	*rpoB*35 ΔlacIZYA oriZ-<cat>* pAM403	RCe585 × pAM403 to Ap^r
JD1133	*ΔlacIZYA recJ284::*Tn*10 ΔrecB::dhfr* pAM375	JD1127 × P1.AM1675 to Tm^r Ap^r
JD1134	*ΔlacIZYA oriZ-<cat> ΔrecB::dhfr Δtus::kan* pAM375	RCe601 × P1.RCe203 to Km^r
JD1137	*ΔlacIZYA oriZ-<cat> Δrep::dhfr* pAM403	JD1129 × P1.RCe371 to Ap^r Tm^r
JD1138	*rpoB*35 ΔlacIZYA oriZ-<cat> Δrep::dhfr* pAM403	JD1130 × P1.RCe371 to Tm^r Ap^r
JD1139	*ΔlacIZYA recJ284::*Tn*10 ΔrecB::dhfr*	plasmid-free derivative of JD1133
JD1140	*ΔlacIZYA oriZ-<cat> ΔrecB::dhfr Δtus::kan*	plasmid-free derivative of JD1134
JD1141	*ΔlacIZYA oriZ-<cat> Δrep::dhfr*	plasmid-free derivative of JD1137
JD1142	*rpoB*35 ΔlacIZYA oriZ-<cat> Δrep::dhfr*	plasmid-free derivative of JD1138
JD1143	*rpoB*35 ΔlacIZYA recB268::*Tn*10*	plasmid-free derivative of N7592
JD1144	*ΔlacIZYA oriZ-<cat> ΔrecB::dhfr*	plasmid-free derivative of RCe601

JD1145	*rpoB*35 ΔlacIZYA oriZ-<cat> ΔrecB::dhfr*	plasmid-free derivative of RCe603
JD1146	*ΔsbcCD::kan ΔrecB::dhfr*	RCe562 × P1.AM1675 to Tm^r
JD1147	*ΔxonA::apra ΔsbcCD::kan ΔrecB::dhfr*	RCe569 × P1.AM1675 to Tm^r
JD1148	*ΔxonA::apra ΔrecB::dhfr*	RCe563 × P1.AM1675 to Tm^r
JD1150	*ΔxseA::dhfr recB268::*Tn*10*	RCe564 × P1.N7592 to Tc^r
JD1181	*ΔlacIZYA pheA::oriX-cat*	TB28 × P1.RUC1593 to Cm^r
JD1185	*ΔlacIZYA pheA::oriX-cat* pAM375	JD1181 × pAM375 to Ap^r
JD1190	*rpoB*35 ΔlacIZYA pheA::oriX-cat*	N5925 × P1.RUC1593 to Cm^r
JD1191	*ΔlacIZYA pheA::oriX-cat ΔrecB::dhfr* pAM375	JD1185 × P1.AM1675 to Tm^r Ap^r
JD1195	*rpoB*35 ΔlacIZYA pheA::oriX-cat* pAM375	JD1190 × pAM375 to Ap^r
JD1199	*rpoB*35 ΔlacIZYA pheA::oriX-cat ΔrecB::dhfr* pAM375	JD1195 × P1.AM1675 to Tm^r Ap^r
JD1252	*ΔhipA728::<kan>*	MG1655 × P1.JW1500-2 to Km^r
JD1269	*ΔlacIZYA ΔrecB::dhfr*	TB28 × P1.AM1675 to Tm^r
JD1270	*ΔhipB729::<kan>*	MG1655 × P1.JW1501 to Km^r
JD1286	*tos+200kb-kan ΔrecB::dhfr*	BW66 × P1.AM1675 to Tm^r
JD1294	*ΔhipB729::<kan> ΔrecB::dhfr*	JD1270 × P1.AM1675 to Tm^r
JD1297	*tos+200kb-kan ΔrecB::dhfr Δtus::cat*	JD1286 × P1.AM1775 to Cm^r
JD1301	*ΔhipA728::<kan> ΔrecB::dhfr*	JD1252 × P1.AM1675 to Tm^r
JD1306	*tos+200kb-kan ΔrecB::dhfr Δtus::cat* N15 lysogen	JD1297 × N15 to N15^r
JD1318	*rpoB*35 ΔlacIZYA oriZ-<cat> recB268::*Tn*10* pAM375	RCe598 × P1.N4278 to Tc^r Ap^r
JD1321	*ΔlacIZYA oriZ-<cat> recB268::*Tn*10* pAM375	RCe597 × P1.N4278 to Tc^r Ap^r
JD1322	*rpoB*35 ΔlacIZYA oriZ-<cat> recB268::*Tn*10 tus1::dhfr* pAM375	JD1318 × P1.N6798 to Tm^r Ap^r
JD1325	*rpoB*35 ΔlacIZYA oriZ-<cat> Δrep::dhfr ΔoriC::kan^b* pAM403	JD1138 × P1.RCe576 to Km^r Ap^r
JD1326	*ΔlacIZYA oriZ-<cat> recB268::*Tn*10 tus1::dhfr* pAM375	JD1321 × P1.N6798 to Tm^r Ap^r
JD1330	*rpoB*35 ΔlacIZYA oriZ-<cat> recB268::*Tn*10 tus1::dhfr ΔoriC::kan^b* pAM375	JD1322 × P1.RCe576 to Km^r Ap^r
JD1331	*ΔlacIZYA oriZ-<cat> recB268::*Tn*10 tus1::dhfr ΔoriC::kan^b* pAM375	JD1326 × P1.RCe576 to Km^r Ap^r
JD1337	*ΔlacIZYA oriZ-<cat> Δrep::dhfr ΔoriC::kan^b* pAM403	JD1137 × P1.JD1325 to Km^r Ap^r
JD1344	*ΔlacIZYA pheA::oriX-cat ΔrecB::dhfr*	Plasmid-free derivative of JD1191
JD1345	*rpoB*35 ΔlacIZYA pheA::oriX-cat ΔrecB::dhfr*	Plasmid-free derivative of JD1199
JD1359	*tos-kan Δtus::cat*	RCe427 × P1.AM1775 to Cm^r
JD1367	*tos-kan Δtus::cat ΔrecB::dhfr*	JD1359 × P1.AM1675 to Tm^r
JD1371	*tos-kan Δtus::cat ΔrecB::dhfr* N15 lysogen	JD1367 × N15 to N15^r
JD1412	*rpoB*35 ΔlacIZYA ΔsbcCD::kan*	N5925 × P1.RCe562 to Km^r
JD1422	*rpoB*35 ΔlacIZYA ΔsbcCD::kan recB268::*Tn*10*	JD1412 × P1.N4278 to Tc^r
JD1428	*oriZ-<cat> ΔsbcCD::kan*	RCe504 × P1.RCe562 to Km^r
JD1429	*oriZ-<cat> ΔsbcCD::kan recB268::*Tn*10*	JD1428 × P1.N4278 to Tc^r

JJ1359	*ΔlacIZYA dam1::kan ΔrecG::apra tus1::dhfr*	[7]
N4278	*recB268::*Tn*10*	[9]
N4560	*ΔrecG265::cat*	[9]
N4934	*recJ284::*Tn*10*	[10]
N5286	*xonAΔ300::cat*	MG1655 × P1.STL2694 to Cm^r
N5296	*xonAΔ300::cat ΔsbcCD::kan*	N5286 × P1.DL729 to Km^r
N5925	*rpoB*35 ΔlacIZYA*	[11]
N5960	*priA300 ΔlacIZYA Δrep::kan* pAM374	[5]
N6539	*ΔlacIZYA Δrep::kan* pAM403	[11]
N6798	*ΔrecG265::cat tus1::dhfr*	N4560 × P1.JJ1359 to Tm^r
N7582	*rpoB*35 ΔlacIZYA* pAM375	N5925 × pAM375 to Ap^r
N7592	*rpoB*35 ΔlacIZYA recB268::*Tn*10* pAM375	N7582 × P1.TRM308 to Tc^r Ap^r
N7684	*ΔlacIZYA ΔsbcCD::spc ΔxseA::dhfr ΔxonA::apra* pAM401	[12]
RCe203	*tnaA::*Tn*10 dnaA46 Δtus::kan*	[7]
RCe371	*Δrep::dhfr* pDIM113	AM1969 × pDIM113 to Ap^r
RCe395	*rpoB*35 tnaA::*Tn*10 dnaA46 ΔrnhA::cat tus1::dhfr ΔoriC::kan*^{b}	[7]
RCe427	*tos-kan*	[7]
RCe504	*oriZ-<cat>*	[2]
RCe544	*ΔlacIZYA oriZ-<cat>*	[2]
RCe562	*ΔsbcCD::kan*	MG1655 × P1.N5296 to Km^r
RCe563	*ΔxonA::apra*	MG1655 × P1.N7684 to Apra^r
RCe567	*oriZ-<cat> tus1::dhfr*	[2]
RCe569	*ΔxonA::apra ΔsbcCD::kan*	RCe563 × P1.N5296 to Km^r
RCe576	*rpoB*35 oriZ-<cat> tus1::dhfr ΔoriC::kan*^{b}	[2]
RCe585	*rpoB*35 ΔlacIZYA oriZ-<cat>*	N5925 × P1.RCe544 to Cm^r
RCe597	*ΔlacIZYA oriZ-<cat>* pAM375	RCe544 × pAM375 to Ap^r
RCe598	*rpoB*35 ΔlacIZYA oriZ-<cat>* pAM375	RCe585 × pAM375 to Ap^r
RCe601	*ΔlacIZYA oriZ-<cat> ΔrecB::dhfr* pAM375	RCe597 × P1.AM1675 to Tm^r
RCe603	*rpoB*35 ΔlacIZYA oriZ-<cat> ΔrecB::dhfr* pAM375	RCe598 × P1.AM1675 to Tm^r
RCe613	*rpoB*35 ΔlacIZYA oriZ-<cat> ΔrecB::dhfr ΔoriC::kan*^{b} pAM375	RCe603 × RCe395 to Km^r
SLM1092	*tos-kan*	MG1655 × P1.RCe427 to Km^r
SLM1093	*tos-kan ΔrecB::dhfr*	SLM1092 × P1.AM1675 to Tm^r
SLM1100	*tos-kan ΔrecB::dhfr* N15 lysogen	SLM1093 × N15 to N15^r
SLM1103	*ΔrecB::dhfr* N15 lysogen	AM1675 × N15 to N15^r
TRM308	*ΔargE::I-SceI*^{cs} *recB268::*Tn*10 sbcA*	[5]
TB28	*ΔlacIZYA*	[13]

a – Only the relevant additional genotype of the derivatives is shown. The abbreviations *apra*, *kan*, *cat* and *dhfr* refer to insertions conferring resistance to apramycin (Apra^r), kanamycin (Km^r), chloramphenicol (Cm^r) and trimethoprim (Tm^r), respectively. Tn*10* indicates the presence of a transposon 10 integration, which confers resistance to tetracyclin (Tc^r). '<>' indicates the use of *frt* sites, where *frt* stands for the 34 bp recognition site of the FLP/*frt* site-directed recombination system. Thus, *<kan>* refers to a kanamycin marker flanked by an *frt* site either side. *tos* refers to the telomerase occupancy site from the bacteriophage N15 genome followed by a kanamycin resistance cassette [8]. The

term "× N15 to N15r" refers to isolation of *E. coli* cells lysogenized with bacteriophage N15. These cells can be identified by their resistance to re-infection with N15 (see Supplementary Methods). All plasmids are described and cited in Supplementary Methods.

b – *ΔoriC* refers to a replacement of the entire origin region (754 bp) including DnaA boxes and 13mers as well as the entire *mioC* gene by a kanamycin resistance cassette [7].

c – Coli Genetic Stock Center, Yale University.

SUPPLEMENTARY FIGURE LEGENDS

Suppl. Figure 1. Linearisation of the *Escherichia coli* chromosome. **A)** Schematic representation of the *tosRL* processing by the bacteriophage N15 telomerase TelN. **B)** Schematic representation of the area around the *aroH* gene, 200 kb from the *dif* dimer resolution site, with and without integrated *tosRL-kan* site. The linearisation verification primers are shown in green (for primer sequences see [8]) and the PCR product sizes in wild type cells und integrants are indicated. **C)** PCR products generated with the linearisation verification primers for wild type cells lysogenized with phage N15 (lane 1), *tos+200kb-kan* cells (lane 2) and two *tos+200kb-kan* constructs lysogenized with phage N15 (lanes 3 & 4). The shift of the PCR product size in lane 2 indicates the presence of the *tos+200kb-kan* cassette. Linearisation of the chromosome (lanes 3 & 4) prevents formation of a PCR product since the chromosome is interrupted between the primer binding sites. The absence of a detectable PCR product confirms that the amount of circular chromosomes unprocessed by TelN in the population is very low, as reported [8]. **D–G)** Verification of chromosome linearisation by pulse field gel electrophoresis. Processing of the *tos+200kb-kan* cassette by TelN splits the 250.16 kb *Not*I fragment between positions 1,611,219 and 1,861,382 into a 175.16 and a 75 kb fragment (G). This can be easily detected via pulse field gel electrophoresis (D–F). Both the 175.16 kb and the 75 kb fragment are absent in cells containing only the *tos+200kb-kan* cassette (lane 1), but become detectable in two separate constructs upon phage N15 lysogenic infection (lanes 2 & 3).

Suppl. Figure 2. Activity of an ectopic replication origin in the left-hand replichore is reduced in the absence of RecBCD due to replication-transcription conflicts. The replication profiles are generated by plotting the number of sequence reads (normalised against reads for a stationary phase wild type control) against their chromosomal location. The schematic representation of the *E. coli* chromosome above each panel shows positions of the two origins, *oriC* and *oriX,* and *ter* sites (above) as well as the *dif* chromosome dimer resolution site and *rrn* operons A–E, G and H (below). The strains used were JD1181 (*oriC*$^+$ *oriX*$^+$), JD1344 (*oriC*$^+$ *oriX*$^+$ *ΔrecB*) and JD1345 (*oriC*$^+$ *oriX*$^+$ *ΔrecB rpoB*35*).

Suppl. Figure 3. Cell sizes of wild type and *ΔrecB* cells grown in LB broth. For all strains samples from fresh overnight cultures grown in LB broth were diluted 100-fold in fresh LB broth and incubated with vigorous aeration until an A_{600} reached 0.48 at 37°C to ensure they

were in exponential growth conditions. Cells were transferred onto a slide covered with an agarose pad and the slides examined using a Nikon T*i*-U inverted microscope equipped with a DS-Qi2 camera (Nikon). Images were taken and cell lengths of 150 cells per strain analysed via Nikon NIS-Elements Br software 4.3 (Nikon).

REFERENCES

[1] S.E. Luria, J.W. Burrous, Hybridization between *Escherichia coli* and Shigella, J. Bacteriol. 74 (1957) 461–476.

[2] D. Ivanova, T. Taylor, S.L. Smith, J.U. Dimude, A.L. Upton, M.M. Mehrjouy, O. Skovgaard, D.J. Sherratt, R. Retkute, C.J. Rudolph, Shaping the landscape of the *Escherichia coli* chromosome: replication-transcription encounters in cells with an ectopic replication origin, Nucleic Acids Res. 43 (2015) 7865–7877. doi:10.1093/nar/gkv704.

[3] C.A. Müller, M. Hawkins, R. Retkute, S. Malla, R. Wilson, M.J. Blythe, R. Nakato, M. Komata, K. Shirahige, A.P.S. de Moura, C.A. Nieduszynski, The dynamics of genome replication using deep sequencing, Nucleic Acids Res. 42 (2014) e3. doi:10.1093/nar/gkt878.

[4] O. Skovgaard, M. Bak, A. Løbner-Olesen, N. Tommerup, Genome-wide detection of chromosomal rearrangements, indels, and mutations in circular chromosomes by short read sequencing, Genome Res. 21 (2011) 1388–1393. doi:10.1101/gr.117416.110.

[5] A.A. Mahdi, C. Buckman, L. Harris, R.G. Lloyd, Rep and PriA helicase activities prevent RecA from provoking unnecessary recombination during replication fork repair, Genes Dev. 20 (2006) 2135–2147. doi:10.1101/gad.382306.

[6] Bachmann, B J, Derivations and Genotypes of Some Mutant Derivatives of *Escherichia coli* K-12, in: *Escherichia Coli* Salmonella Cell. Mol. Biol., Second Edition, ASM Press, 1996.

[7] C.J. Rudolph, A.L. Upton, A. Stockum, C.A. Nieduszynski, R.G. Lloyd, Avoiding chromosome pathology when replication forks collide, Nature. 500 (2013) 608–611. doi:10.1038/nature12312.

[8] T. Cui, N. Moro-oka, K. Ohsumi, K. Kodama, T. Ohshima, N. Ogasawara, H. Mori, B. Wanner, H. Niki, T. Horiuchi, *Escherichia coli* with a linear genome, EMBO Rep. 8 (2007) 181–187. doi:10.1038/sj.embor.7400880.

[9] T.R. Meddows, A.P. Savory, R.G. Lloyd, RecG helicase promotes DNA double-strand break repair, Mol. Microbiol. 52 (2004) 119–132. doi:10.1111/j.1365-2958.2003.03970.x.

[10] C.J. Rudolph, A.L. Upton, R.G. Lloyd, Maintaining replication fork integrity in UV-irradiated *Escherichia coli* cells, DNA Repair. 7 (2008) 1589–1602. doi:10.1016/j.dnarep.2008.06.012.

[11] C.P. Guy, J. Atkinson, M.K. Gupta, A.A. Mahdi, E.J. Gwynn, C.J. Rudolph, P.B. Moon, I.C. van Knippenberg, C.J. Cadman, M.S. Dillingham, R.G. Lloyd, P. McGlynn, Rep provides a second motor at the replisome to promote duplication of protein-bound DNA, Mol. Cell. 36 (2009) 654–666. doi:10.1016/j.molcel.2009.11.009.

[12] C.J. Rudolph, A.A. Mahdi, A.L. Upton, R.G. Lloyd, RecG protein and single-strand DNA exonucleases avoid cell lethality associated with PriA helicase activity in *Escherichia coli*, Genetics. 186 (2010) 473–492. doi:10.1534/genetics.110.120691.

[13] T.G. Bernhardt, P.A.J. de Boer, The *Escherichia coli* amidase AmiC is a periplasmic septal ring component exported via the twin-arginine transport pathway, Mol. Microbiol. 48 (2003) 1171–1182.

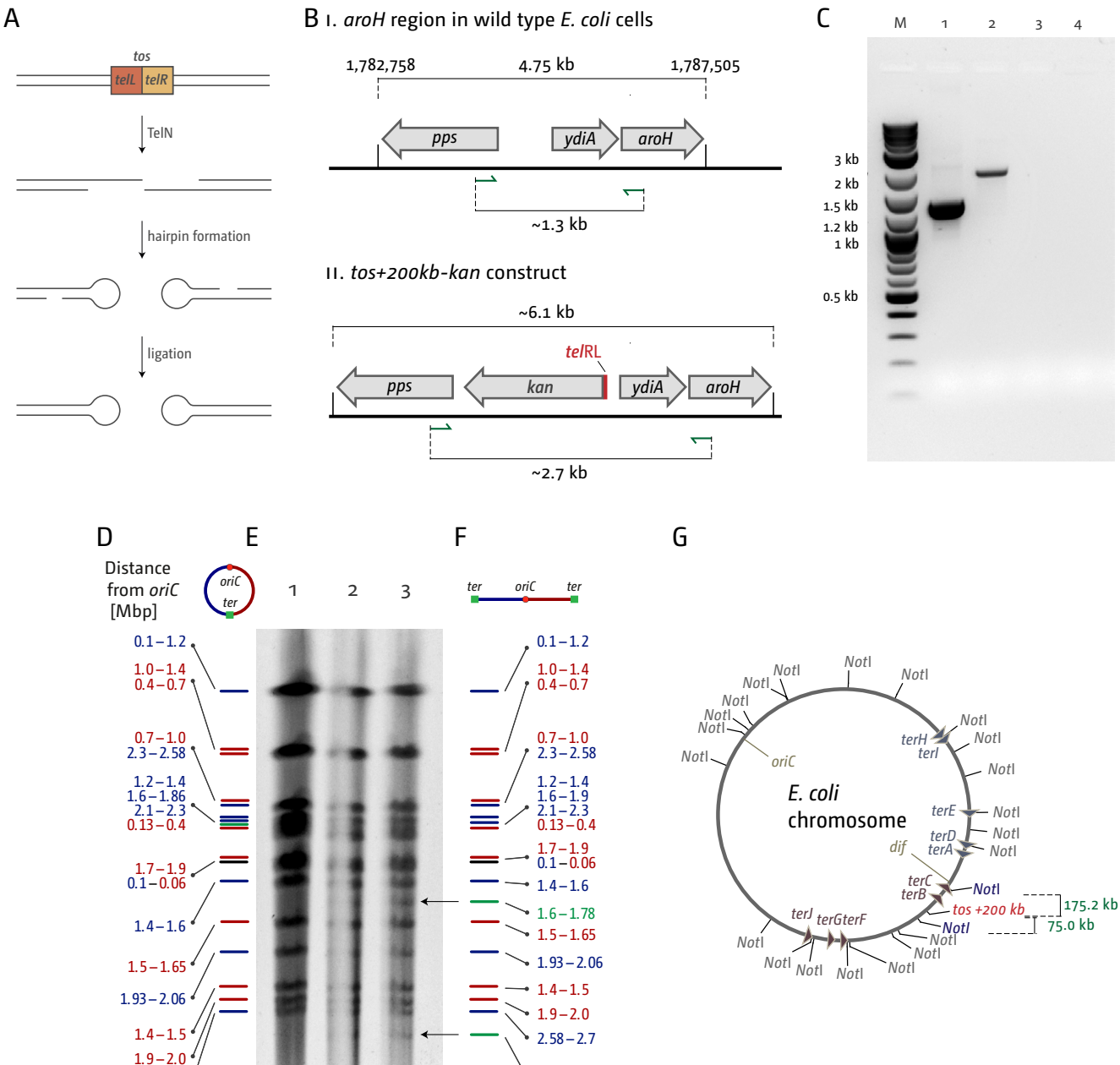

Dimude *et al.* Figure S1

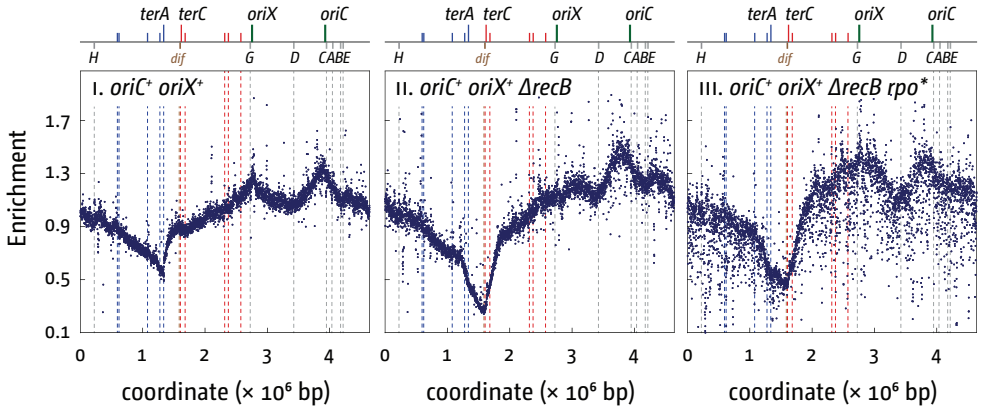

Dimude *et al.*, Supplementary Figure 2

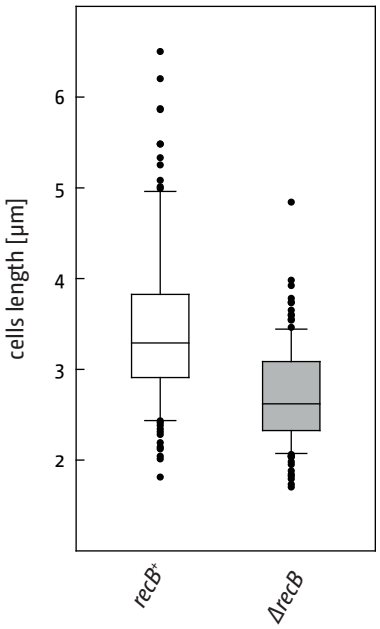

Dimude *et al.*, Supplementary Figure 3